Optical and Quantum Electronics (2023) 55:286
https://doi.org/10.1007/s11082-022-04402-3

Optical soliton solutions and various breathers lump interaction solutions with periodic wave for nonlinear Schrödinger equation with quadratic nonlinear susceptibility

Syed T. R. Rizvi[1] Aly R. Seadawy[2] Samia Ahmed[1] Azhar Bashir[1]

Received: 8 October 2022 / Accepted: 13 November 2022 / Published online: 1 February 2023

Abstract
In this article, we cover some soliton solutions and breathers for nonlinear Schrödinger equation with quadratic nonlinear susceptibility like that Breather lump wave solutions, Interaction between lump periodic and kink wave, lump soliton solution, Lump one kink solution, Lump two kink solution, multiwave solution, periodic cross kink solution, periodic cross lump wave solution, periodic wave solution and rogue wave solution. We also explore some rational solution such as *M*-shaped rational solutions, *M*-shaped rational solutions with one and two kink, kink cross rational solution and periodic cross rational solution. Also, we acquire homoclinic breather solution, *M*-shaped interaction with rogue and kink and *M*-shaped interaction with periodic and kink. Furthermore we also study the stability of our solutions. we also represents our solutions graphically such as 3D, 2D, contour, density plot and stream plot.

Keywords Homoclinic breather · Lump soliton · M-shaped solution · Multiwave · Rogue wave

1 Introduction

The nonlinear Schrödinger equation (NLSE) is essential for the improvement in optical communication system. From the mathematical perspective Schrödinger equation combines the characteristics of both parabolic and hyperbolic equations. The NLSE applied in many scientific fields to explain nonlinear physical characteristics also have applications in variety of fields including semiconductor manufacturing, biology, solid-state physics, condense matter physics, quantum chemistry, nonlinear optics, wave propagation, optical

✉ Aly R. Seadawy
aabdelalim@taibahu.edu.sa

Syed T. R. Rizvi
strrizvi@gmail.com

[1] Department of Mathematics, COMSATS University Islamabad, Lahore Campus, Pakistan

[2] Mathematics Department, Faculty of Science, Taibah University, Al-Madinah Al-Munawarah 41411, Kingdom of Saudi Arabia

communication, protein folding and bending, nano-technology and industry (Ilhan et al. 2022; Li et al. 2022; Mohyaldeen et al. 2022; Yang et al. 2018). At the present time, the study of NLSE including analysis, numerics and applications becoming significant subject in computational and applied mathematics (Shen et al. 2021, 2022; Song et al. 2020; Guo et al. 2020). Some efficient ways for obtaining soliton solutions and optics have grabed the attention of many researchers because soliton theory is the fundamental and exciting topic in research (Rizvi et al. 2021, 2022a, b; Seadawy et al. 2021, 2022a, b, c, d; Batool et al. 2022; Ali et al. 2022; Ashraf et al. 2022).

In this paper, we will study NLSE-QNS given by Biswas et al. (2022):

$$iy_t + c_1 y_{xx} + d_1 y_{xt} + b_1 y + \alpha_1 y^* z = ia_1 y_x, \tag{1}$$

$$iz_t + c_2 z_{xx} + d_2 z_{xt} + b_2 z + \alpha_2 y^2 = ia_2 z_x. \tag{2}$$

where x and t represents the spatial and temporal variables respectively. The coefficients a_j, b_j, c_j, d_j, α_j $(j = 1, 2)$ are real valued constants. a_j are the coefficients of inter-modal dispersion. c_j depict the coefficient of chromatic dispersion, while d_j stands for the coefficient of spatio-temporal dispersion. And α_j are the coefficient of QN. The function $y = y(x, t$ and $z = z(x, t)$ are complex valued function. The functions y represents the wave profile of the forward harmonic waves and z represents second harmonic waves. And $y^* = y^*(x, t)$ is the conjugate of $y = y(x, t)$.

2 LSS

By using following transformation, we obtain solution for LSS Biswas et al. (2022):

$$y(x, t) = 2s(lng)_x, \quad z(x, t) = 2(lnj)_{xx}. \tag{3}$$

We have following bilinear form by putting Eq. (3) into Eq. (1),

$$\begin{aligned} &2b_1 sg^2 j^2 g_x - 2isgj^2 g_t g_x + 2ia_1 sgj^2 g_x^2 + 4d_1 sj^2 g_t g_x^2 + 4c_1 sj^2 g_x^3 - 2\alpha_1 g^3 y^* j_x^2 \\ &+ 2isg^2 j^2 g_{xt} - 4d_1 sgj^2 g_x g_{xt} - 2ia_1 sg^2 j^2 g_{xx} - 2d_1 sgj^2 g_t g_{xx} - 6c_1 sgj^2 g_x g_{xx} \\ &+ 2\alpha_1 g^3 jy^* j_{xx} + 2d_1 sg^2 j^2 g_{xxt} + 2c_1 sg^2 j^2 g_{xxx}. \end{aligned} \tag{4}$$

For LS g and j are the following functions:

$$\begin{aligned} g &= \Lambda_1^2 + \Lambda_2^2 + k_7, \\ j &= \Lambda_1^2 + \Lambda_2^2 + k_8, \end{aligned} \tag{5}$$

where

$$\Lambda_1 = k_1 x + k_2 t + k_3, \quad \Lambda_2 = k_4 x + k_5 t + k_6,$$

where $k_i (1 \le i \le 8)$ are real parameters. Insert Eq. (5) in to Eq. (4). We find some equations that provide coefficient values, including:

$$k_1 = 0, k_3 = 0, k_4 = k_4, k_6 = 0, k_7 = 0, k_8 = 0, k_2 = \frac{4}{3} ia_1 k_4, k_5 = \frac{4a_1 k_4}{3}, \tag{6}$$

To obtain the LSS of Eq. (1), Insert Eq. (6) in to Eq. (5) and then in Eq. (3)

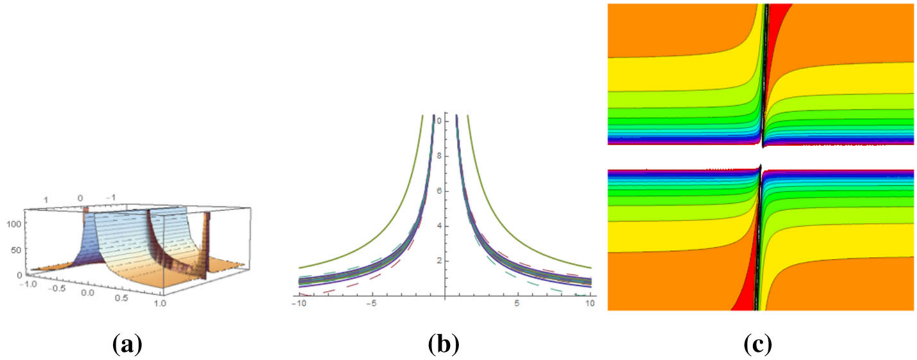

Fig. 1 LS graphs of solution $y(x, t)$ of Eq. (7) are shown as $k_4 = 0.5, s = 4, a_1 = -7$. **a** 3D plot, **b** 2D plot, **c** contour plot

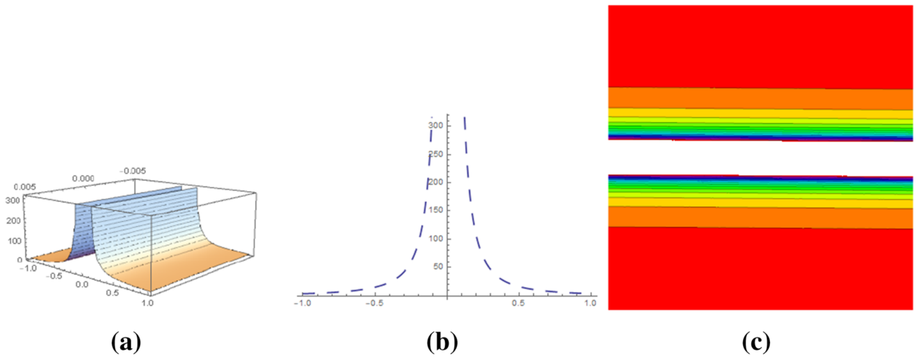

Fig. 2 LS graphs of solution $z(x, t)$ of Eq. (8) are shown as $k_4 = 5, s = 0.4, a_1 = 1.1$.

$$y(x,t) = \frac{4k_4 s\left(\frac{4a_1 k_4 t}{3} + k_4 x\right)}{\left(\frac{4a_1 k_4 t}{3} + k_4 x\right)^2 - \frac{16}{9}a_1^2 k_4^2 t^2}. \tag{7}$$

$$z(x,t) = \frac{2\left(2k_4^2\left(\left(\frac{4a_1 k_4 t}{3} + k_4 x\right)^2 - \frac{16}{9}a_1^2 k_4^2 t^2\right) - 4k_4^2\left(\frac{4a_1 k_4 t}{3} + k_4 x\right)^2\right)}{\left(\left(\frac{4a_1 k_4 t}{3} + k_4 x\right)^2 - \frac{16}{9}a_1^2 k_4^2 t^2\right)^2}. \tag{8}$$

Now we represent some dynamical representation of solutions (Figs. 1 and 2):

3 LOKS

The *LOKS*'s solution, which contains the sum of the quadratic functions and an exponential functions, is obtain in this section for Eq. (1) We use the following function g and j Ren et al. (2019):

$$g = \Lambda_1^2 + \Lambda 2^2 + n_1 e^{H_1} + k_7,$$
$$j = \Lambda_1^2 + \Lambda_2^2 + n_1 e^{H_1} + k_8, \tag{9}$$

where

$$\Lambda_1 = k_1 x + k_2 t + k_3, \quad \Lambda_2 = k_4 x + k_5 t + k_6, \quad H_1 = r_1 x + r_2 t,$$

Inserting Eq. (9) in to Eq. (4). By inserting all the coefficient of the $x, t, e^{4r_1x+4r_2t}, e^{3r_1x+3r_2t}, e^{2r_1x+2r_2t}, e^{r_1x+r_2t}, y^*(x,t), y^*(x,t)e^{4r_1x+4r_2t}, y^*(x,t)e^{3r_1x+3r_2t}$, $y^*(x,t)$ $e^{2r_1x+2r_2t}$, $y^*(x,t)e^{r_1x+r_2t}$ to be zero, we get algebraic expression that provide coefficient values as:

$$k_1 = 0, k_2 = k_2, k_3 = 0, k_4 = -\frac{3\left(k_2^2 - 2k_5^2\right)}{2(k_5(3a_1 + 2b_1d_1))},$$
$$k_5 = k_5, k_6 = k_6, k_7 = k_7, k_8 = k_8, n_1 = n_1, r_1 = 0, r_2 = \frac{1}{3}(-(4i))b_1, \tag{10}$$

putting Eq. (10) in to Eq. (9) and then in Eq. (3) to get *LOKS* of Eq. (1),

$$y(x,t) = -\frac{6s\left(k_2^2 - 2k_5^2\right)\left(-\frac{3x\left(k_2^2-2k_5^2\right)}{2k_5(3a_1+2b_1d_1)} + k_5t + k_6\right)}{k_5(3a_1 + 2b_1d_1)\left(\left(-\frac{3x\left(k_2^2-2k_5^2\right)}{2k_5(3a_1+2b_1d_1)} + k_5t + k_6\right)^2 + n_1 e^{\frac{1}{3}(-4)ib_1t} + k^2t^2 + k_7\right)}. \tag{11}$$

$$z(x,t) = \frac{2\left(-\frac{9\left(k_2^2-2k_5^2\right)^2\Psi^2}{k_5^2(3a_1+2b_1d_1)^2} + \frac{9\left(k_2^2-2k_5^2\right)^2\left(\Psi^2+n_1e^{\frac{1}{3}(-4)ib_1t}+k_2^2t^2+k_8\right)}{2k_5^2(3a_1+2b_1d_1)^2}\right)}{\left(\Psi^2 + n_1e^{\frac{1}{3}(-4)ib_1t} + k_2^2t^2 + k_8\right)^2}, \tag{12}$$

where $\Psi = -\frac{3x\left(k_2^2-2k_5^2\right)}{2k_5(3a_1+2b_1d_1)} + k_5t + k_6$.

Now we represent some graphical representation of solutions (Figs. 3 and 4):

4 LTKS

The *LTKS*'s solution, which contains the sum of the quadratic functions and an exponential functions, is obtain in this section for Eq. (1). We use the following function g and j:

$$g = \Lambda_1^2 + \Lambda_2^2 + n_1e^{H_1} + n_2e^{H_2} + k_7,$$
$$j = \Lambda_1^2 + \Lambda_2^2 + n_1e^{H_1} + n_2e^{H_2} + k_8, \tag{13}$$

where

$$\Lambda_1 = k_1x + k_2t + k_3, \quad \Lambda_2 = k_4x + k_5t + k_6, \quad H_1 = r_1x + r_2t, \quad H_2 = r_3x + r_4t,$$

Putting Eq. (13) in to Eq. (4). By putting all the coefficient of the $x, t, e^{r_1x+r_2t}, e^{2r_1x+2r_2t}, e^{3r_1x+3r_2t}, e^{4r_1x+4r_2t}, e^{r_3x+r_4t}, e^{2r_3x+2r_4t}, e^{3r_3x+3r_4t}, e^{r_1x+r_2t+r_3x+r_4t}$, $e^{2r_1x+2r_2t}$ $+r_3x + r_4t, e^{3r_1x+3r_2t+r_3x+r_4t}, e^{r_1x+r_2t+2r_3x+2r_4t}, e^{2r_1x+2r_2t+2r_3x+2r_4t}, e^{r_1x+r_2t+3r_3x+3r_4t}, y^*(x,t)$ e^{r_1x}

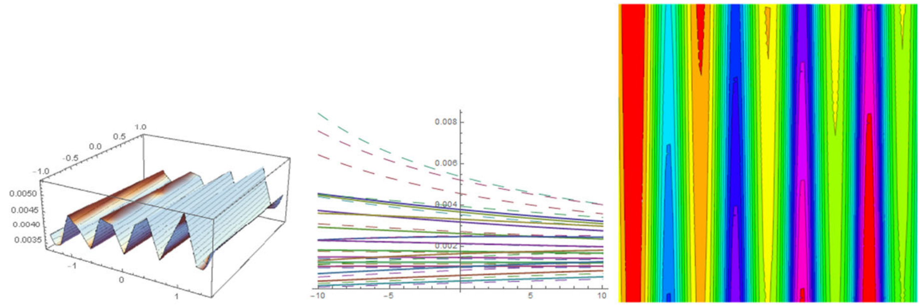

(a) (b) (c)

Fig. 3 *LOKS* dynamical representation of solution $y(x, t)$ of Eq. (11) are shown as $a_1 = 1.5, b_1 = 7, d_1 = 0.9, k_2 = 0.5, k_5 = 0.2, k_6 = -4, k_7 = -2, n_1 = 2.2, s = 0.05$

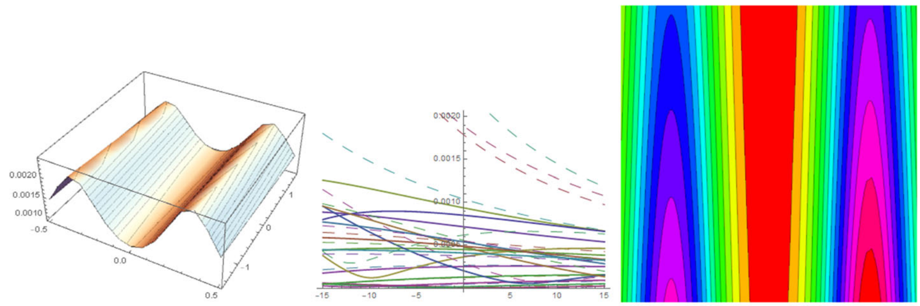

(a) (b) (c)

Fig. 4 *LOKS* graphical representation of solution $z(x, t)$ of Eq. (12) are shown as $a_1 = 1.5, b_1 = 7, d_1 = 0.9, k_2 = 0.5, k_5 = 0.2, k_6 = -4, k_7 = -2, k_8 = -0.07, n_1 = 2.2, s = 0.05$

$+r_2t, y^*(x,t) \quad e^{2r_1x+2r_2t}, y^*(x,t)e^{3r_1x+3r_2t}, y^*(x,t)e^{4r_1x+4r_2t}, y^*(x,t) \quad e^{r_3x+r_4t}, y^*(x,t)e^{2r_3x+2r_4t}$, $y^*(x,t)e^{3r_3x+3r_4t}, y^*(x,t)e^{r_1x+r_2t+r_3x+r_4t}, y^*(x,t) \quad e^{2r_1x+2r_2t+r_3x+r_4t}, y^*(x,t) \quad e^{3r_1x+3r_2t+r_3x} \quad +r_4t$, $y^*(x,t)e^{r_1x+r_2t+2r_3x+2r_4t}, y^*(x,t)e^{2r_1x+2r_2t+2r_3x+2r_4t}, y^*(x,t)e^{r_1x+r_2t+3r_3x+3r_4t}$ to be zero, we get algebraic expression that provide coefficient values as:

$$k_1 = k_1, k_2 = 0, k_3 = k_3, k_4 = k_4, k_5 = -\frac{2k_4\left(3a_1k_1^2 + 3a_1k_4^2 + 2b_1d_1k_1^2 + 2b_1d_1k_4^2\right)}{3\left(k_1^2 - 2k_4^2\right)},$$
$$k_6 = 0, k_7 = k_7, k_8 = 0, n_1 = n_1, n_2 = n_2, r_1 = r_1, r_2 = \frac{1}{2}i(-4b_1 + ir_4), r_3 = 0, r_4 = r_4, \tag{14}$$

Insert Eq. (14) in to Eq. (13) and then in Eq. (3) to get the *LTKS* solution of Eq. (1),

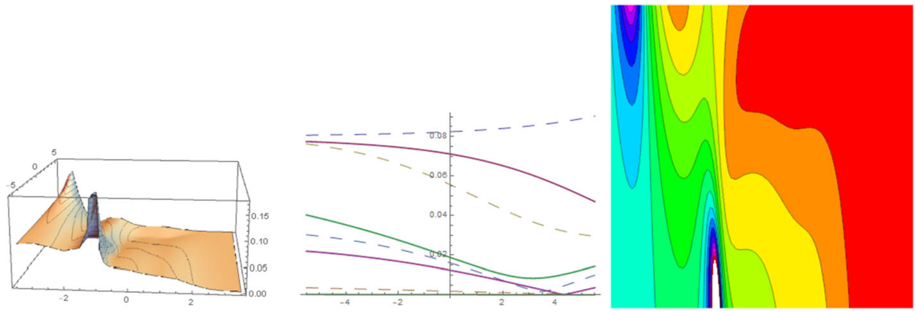

(a) **(b)** **(c)**

Fig. 5 *LTKS* graphical representation of solution $y(x,\ t)$ of Eq. (15) are shown as $k_1 = 0.1, k_3 = -5$, $k_4 = -0.4, k_7 = 3.9, r_1 = -0.2, r_4 = 3, b_1 = 1.5, a_1 = -4, n_1 = 2.5, n_2 = 0.2, d_1 = 3.1, s = -0.2$

$$y(x,t) = \frac{2s\left(2k_4\left(k_4x - \frac{2k_4t\left(3a_1k_1^2+3a_1k_4^2+2b_1d_1k_1^2+2b_1d_1k_4^2\right)}{3\left(k_1^2-2k_4^2\right)}\right) + n_1r_1e^{r_1x+\frac{1}{2}it(-4b_1+ir_4)} + 2k_1(k_1x+k_3)\right)}{\left(k_4x - \frac{2k_4t\left(3a_1k_1^2+3a_1k_4^2+2b_1d_1k_1^2+2b_1d_1k_4^2\right)}{3\left(k_1^2-2k_4^2\right)}\right)^2 + n_1e^{r_1x+\frac{1}{2}it(-4b_1+ir_4)} + (k_1x+k_3)^2 + k_7 + n_2e^{r_4t}}. \tag{15}$$

$$z(x,t) = \frac{2\left(\left(\Phi + 2k_1^2 + 2k_4^2\right)(\Pi) - \left(2k_4(\Pi) + \Phi + 2k_1(k_1x+k_3)\right)^2\right)}{(\Pi)^2}, \tag{16}$$

where $\Phi = n_1r_1^2e^{r_1x+\frac{1}{2}it(-4b_1+ir_4)}$, $\Pi = \left(k_4x - \frac{2k_4t\left(3a_1k_1^2+3a_1k_4^2+2b_1d_1k_1^2+2b_1d_1k_4^2\right)}{3\left(k_1^2-2k_4^2\right)}\right)^2 + \Phi + (k_1x + k_3)^2 + n_2e^{r_4t}$. and

Now we have shown some graphical representation of above solutions (Figs. 5 and 6):

5 RWS

The *RWS*'s solution, which contains the sum of the quadratic functions and an exponential functions, is obtain in this section for Eq. (1) We use the following function g and j Ren et al. (2019):

$$\begin{aligned} g &= \Lambda_1^2 + \Lambda_2^2 + n_1\cosh(\lambda) + k_7, \\ j &= \Lambda_1^2 + \Lambda_2^2 + n_1\cosh(\lambda) + k_8, \end{aligned} \tag{17}$$

where

$$\Lambda_1 = k_1x + k_2t + k_3, \quad \Lambda_2 = k_4x + k_5t + k_6, \quad \lambda = r_1x + r_2t,$$

Insert Eq. (17) in to Eq. (4). Inserting all coefficient of $x, t, \cosh(r_1x + r_2t), \cosh^2(r_1x + r_2t), \cosh^3(r_1x + r_2t), \cosh^4(r_1x + r_2t), \cosh^5(r_1x + r_2t), \cosh^6(r_1x + r_2t)$, $\sinh((r_1x + r_2t)$, $\sinh(r_1x + r_2t)\cosh(r_1x + r_2t), \sinh(r_1x + r_2t)\cosh^2(r_1x + r_2t)$, $\sinh(r_1x + r_2t)\cosh^3(r_1x + r_2t), \sinh(r_1x + r_2t)\cosh^4(r_1x + r_2t), \sinh(r_1x + r_2t)\cosh^5(r_1x + r_2t)$, $\sinh^2$

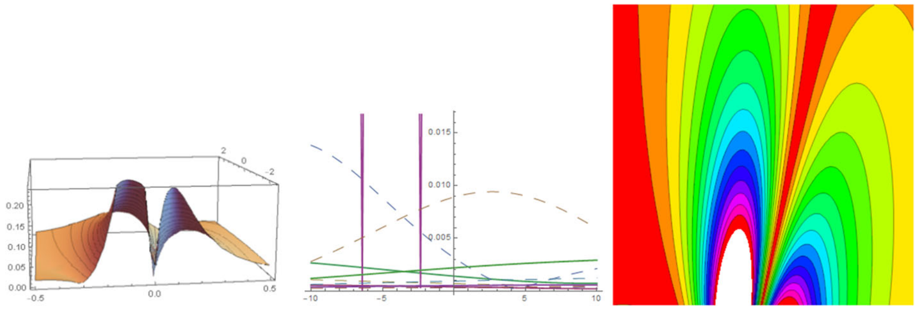

(a) (b) (c)

Fig. 6 *LTKS* graphical representation of solution $z(x, t)$ of Eq. (16) are shown as $k_1 = 1, k_3 = 5, k_4 = 0.4, k_7 = 3, r_1 = 0.2, r_4 = 0.3, b_1 = 5, a_1 = 4, n_1 = 2, n_2 = 0.6, d_1 = 3.5, s = 2.$

$(r_1x + r_2t), \sinh^2(r_1x + r_2t)\ \cosh(r_1x + r_2t), \sinh^2(r_1x + r_2t)\ \cosh^2(r_1x + r_2t), \sinh^2(r_1x + r_2t) \cosh^3(r_1x + r_2t), \sinh^2(r_1x + r_2t)\ \cosh^4(r_1x + r_2t), \sinh^3(r_1x + r_2t), \sinh^3(r_1x + r_2t) \cosh\ (r_1x + r_2t), \sinh^3(r_1x + r_2t) \cosh^2(r_1x + r_2t), \sinh^3(r_1x + r_2t)\ \cosh^3(r_1x + r_2t), y^*(x, t), y^*(x, t)\ \cosh(r_1x + r_2t), y^*(x, t) \cosh^2(r_1x + r_2t), y^*(x, t) \cosh^3(r_1x + r_2t), y^*(x, t) \cosh^4(r_1x + r_2t), y^*(x, t) \cosh^5(r_1x + r_2t), y^*(x, t)\ \cosh^6(r_1x + r_2t), y^*(x, t) \sinh(r_1x + r_2t), y^*(x, t) \sinh(r_1x + r_2t) \cosh(r_1x + r_2t)t), y^*(x, t) \sinh(r_1x + r_2t)\ \cosh^2(r_1x + r_2t), y^* (x, t) \sinh(r_1x + r_2t)\ \cosh^3(r_1x + r_2t), y^*(x, t) \sinh(r_1x + r_2t)\ \cosh^4(r_1x + r_2t), y^*(x, t) \sinh(r_1x + r_2t) \cosh^5(r_1x + r_2t), y^*(x, t)\ \sinh^2(r_1x + r_2t), y^*(x, t) \sinh^2(r_1x + r_2t) \cosh (r_1x + r_2t), y^*(x, t)\ \sinh^2(r_1x + r_2t) \cosh^2(r_1x + r_2t), y^*(x, t) \sinh^2(r_1x + r_2t) \cosh^3\ (r_1x + r_2t), y^*(x, t) \sinh^2(r_1x + r_2t)\ \cosh^4(r_1x + r_2t), y^*(x, t) \sinh^3(r_1x + r_2t), y^*(x, t) \sinh^3(r_1x + r_2t) \cosh(r_1x + r_2t), y^*(x, t) \sinh^3(r_1x + r_2t)\ \cosh^2(r_1x + r_2t), y^*(x, t) \sinh^3(r_1x + r_2t) \cosh^3 (r_1x + r_2t)$ to be zero, we get expression that provide coefficient values as:

$$k_1 = 0, k_2 = -\frac{(3i)k_3(2a_1d_1 + 3c_1)}{4d_1^2}, k_3 = k_3, k_4 = k_4, k_5 = 0, k_6 = 0, k_7 = 0, k_8 = k_8, n_1 = n_1, r_1 = -\frac{2d_1r_2}{3c_1}, r_2 = r_2, \tag{18}$$

Insert Eq. (18) in to Eq. (17) and then in Eq. (3) to have the *RWS* solution of Eq. (1),

$$y(x,t) = \frac{2s\left(2k_4^2x - \frac{2d_1n_1r_2\sinh\left(r_2t - \frac{2d_1r_2x}{3c_1}\right)}{3c_1}\right)}{\left(k_3 - \frac{3ik_3t(2a_1d_1+3c_1)}{4d_1^2}\right)^2 + n_1\cosh\left(r_2t - \frac{2d_1r_2x}{3c_1}\right) + k_4^2x^2}. \tag{19}$$

$$z(x,t) = \frac{2\left(-\left(2k_4^2x - \frac{2d_1n_1r_2\sinh(\Omega)}{3c_1}\right)^2 + \left(\frac{4d_1^2n_1r_2^2\cosh(\Omega)}{9c_1^2} + 2k_4^2\right)(\Upsilon)\right)}{(\Upsilon)^2}, \tag{20}$$

where $\Omega = r_2t - \frac{2d_1r_2x}{3c_1}$ and $\Upsilon = \left(k_3 - \frac{3ik_3t(2a_1d_1+3c_1)}{4d_1^2}\right)^2 + n_1\cosh(\Omega) + k_4^2x^2 + k_8$.

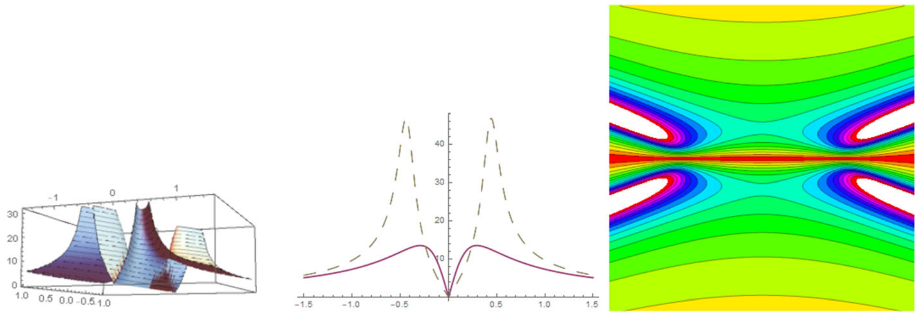

(a) (b) (c)

Fig. 7 *RWS* graphical representation of solution $y(x, t)$ of Eq. (19) are shown as $k_3 = 0.5, k_4 = 7, r_2 = 0.1, c_1 = 5.5, a_1 = 0.06, n_1 = 4, d_1 = 1.3, s = 2.$

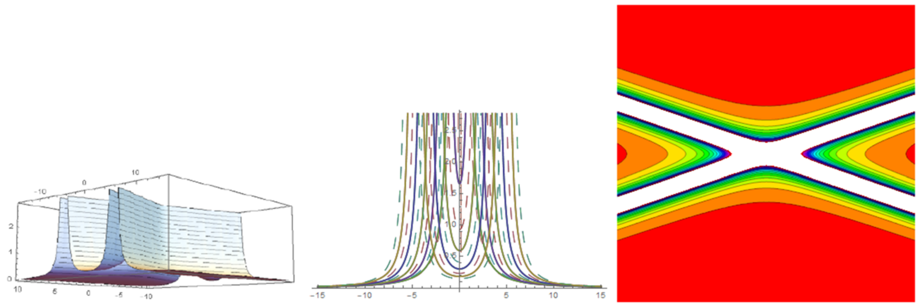

(a) (b) (c)

Fig. 8 *RWS* graphical representation of solution $z(x, t)$ of Eq. (20) are shown as $k_3 = -0.5, k_4 = 7, k_8 = 0.8, r_2 = -0.1, c_1 = -5.5, a_1 = 0.06, n_1 = 0.04, d_1 = 1.3, s = -2.$

Now we have given some graphical representation of these solutions (Figs. 7 and 8):

6 PWS

The *PWS*'s solution, which contains the sum of the quadratic functions and an exponential functions, is obtain in this section for Eq. (1). We use the following function g and j Ren et al. (2019):

$$g = \Lambda_1^2 + \Lambda_2^2 + n_1 \cos(\lambda) + k_7,$$
$$j = \Lambda_1^2 + \Lambda_2^2 + n_1 \cos(\lambda) + k_8, \tag{21}$$

Where

$$\Lambda_1 = k_1 x + k_2 t + k_3, \quad \Lambda_2 = k_4 x + k_5 t + k_6, \quad \lambda = r_1 x + r_2 t,$$

Put Eq. (21) into Eq. (4). The coefficient of $x, t, \cos(r_1 x + r_2 t), \cos^2(r_1 x + r_2 t), \cos^3(r_1 x + r_2 t), \cos^4(r_1 x + r_2 t), \cos^5(r_1 x + r_2 t), \cos^6(r_1 x + r_2 t), \sin(r_1 x + r_2 t), \sin(r_1 x + r_2 t) \cos(r_1 x + r_2 t), \sin(r_1 x + r_2 t) \cos^2(r_1 x + r_2 t), \sin(r_1 x + r_2 t) \cos^3(r_1 x + r_2 t), \sin(r_1 x + r_2 t) \cos^4(r_1 x$

$+r_2t), \sin(r_1x+r_2t) \quad \cos^5(r_1x+r_2t), \sin^2(r_1x+r_2t), \sin^2(r_1x+r_2t)\cos(r_1x+r_2t), \quad \sin^2 (r_1x+r_2t)\cos^2(r_1x+r_2t), \sin^2(r_1x+r_2t)\cos^3(r_1x+r_2t), \quad \sin^2(r_1x+r_2t)\cos^4(r_1x+r_2t), \sin^3(r_1x+r_2t), \sin^3(r_1x+r_2t) \quad \cos(r_1x+r_2t), \sin^3(r_1x+r_2t)\cos^2(r_1x+r_2t), \sin^3(r_1x+ r_2t) \cos^3(r_1x+r_2t), y^*(x,t), y^*(x,t)\cos(r_1x+r_2t), y^*(x,t)\cos^2(r_1x+r_2t), y^*(x,t) \cos^3(r_1x +r_2t), y^*(x,t)\cos^4(r_1x+r_2t), y^*(x,t) \quad \sin(r_1x+r_2t), y^*(x,t)\sin(r_1x+r_2t) \quad \cos(r_1x+r_2t), y^*(x,t) \quad \sin(r_1x+r_2t)\cos^2(r_1x+r_2t), y^*(x,t)\sin(r_1x+r_2t) \quad \cos^3(r_1x+r_2t), y^*(x,t)\sin^2 (r_1x+r_2t), \quad y^*(x,t)\sin^2(r_1x+r_2t)\cos(r_1x+r_2t), y^*(x,t)\sin^2(r_1x+r_2t)\cos^2(r_1x+r_2t)$ values of the parameters which are given below:

$$k_1=0, k_2=k_2, k_3=0, k_4=\frac{k_2^2+2k_5^2}{2(a_1k_5)}, k_5=k_5, k_6=0, k_7=0, k_8=0, \\ n_1=n_1, r_1=0, r_2=r_2, \tag{22}$$

Insert Eq. (22) in to Eq. (21) and then in Eq. (3) to have the *PWS* solution of Eq. (1),

$$y(x,t)=\frac{2s\left(k_2^2+2k_5^2\right)\left(\frac{x\left(k_2^2+2k_5^2\right)}{2a_1k_5}+k_5t\right)}{a_1k_5\left(\left(\frac{x\left(k_2^2+2k_5^2\right)}{2a_1k_5}+k_5t\right)^2+k_2^2t^2+n_1\cos(r_2t)\right)}. \tag{23}$$

$$z(x,t)=\frac{2\left(\frac{\left(k_2^2+2k_5^2\right)^2\left(\left(\frac{x\left(k_2^2+2k_5^2\right)}{2a_1k_5}+k_5t\right)^2+k_2^2t^2+n_1\cos(r_2t)\right)}{2a_1^2k_5^2}-\frac{\left(k_2^2+2k_5^2\right)^2\left(\frac{x\left(k_2^2+2k_5^2\right)}{2a_1k_5}+k_5t\right)^2}{a_1^2k_5^2}\right)}{\left(\left(\frac{x\left(k_2^2+2k_5^2\right)}{2a_1k_5}+k_5t\right)^2+k_2^2t^2+n_1\cos(r_2t)\right)^2}. \tag{24}$$

Now we have some graphical representation of these solutions (Figs. 9 and 10):

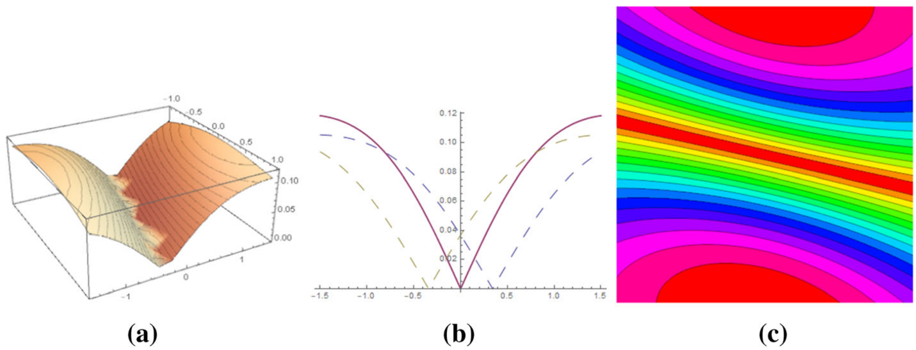

Fig. 9 *PWS* graphical representation of solution $y(x, t)$ of Eq. (23) are shown as $k_2=1.3, k_5=0.5, r_2=0.05, n_1=6, a_1=1.5, s=0.1$.

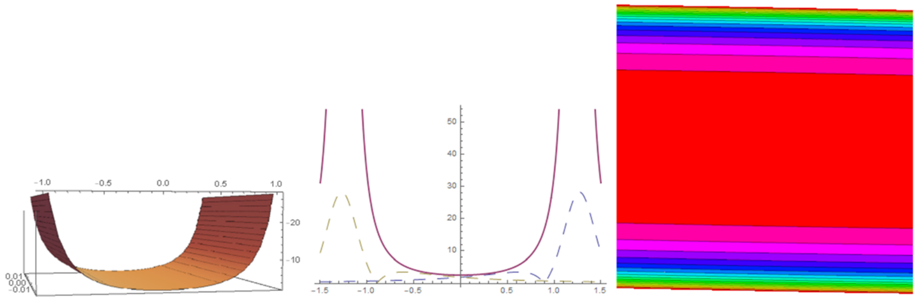

(a) **(b)** **(c)**

Fig. 10 *PWS* graphical representation of solution $z(x, t)$ of Eq. (24) are shown as $k_2 = 1.5, k_5 = 2.5, r_2 = 5, n_1 = -6, a_1 = 1.5, s = 0.1$.

7 PCKS

The *PCKS*'s solution, which contains the sum of the quadratic functions and an exponential functions, is obtain in this section for Eq. (1). We use the following function g and j:

$$\begin{aligned} g &= e^{-\Lambda_1} + r_1 e^{\Lambda_1} + r_2\cos(\Lambda_2) + r_3\cosh(\Lambda_3) + k_{10}, \\ j &= e^{-\Lambda_1} + \kappa_1 e^{\Lambda_1} + \kappa_2\cos(\Lambda_2) + \kappa_3\cosh(\Lambda_3) + k_{11}, \end{aligned} \tag{25}$$

Where

$$\Lambda_1 = k_1x + k_2t + k_3, \quad \Lambda_2 = k_4x + k_5t, \quad \Lambda_3 = k_6x + k_7t,$$

Put Eq. (25) into Eq. (4). We have values of the parameters which are given below:

$$\begin{aligned} &k_1 = 0, k_2 = k_2, k_3 = 0, k_4 = k_4, k_5 = -\frac{c_1k_4}{d_1}, k_6 = k_6, k_7 = 0, k_{10} = k_{10}, k_{11} = -\frac{\kappa_2k_{10}}{r_2} \\ &r_1 = 0, r_2 = r_2, r_3 = r_3, \kappa_1 = 0, \kappa_2 = \kappa_2, \kappa_3 = \kappa_3, \end{aligned} \tag{26}$$

Insert Eq. (26) into Eq. (25) and then in Eq. (3) to have the *PCKS* solution of Eq. (1),

$$y(x,t) = \frac{2k_4r_2s\sin\left(\frac{c_1k_4t}{d_1} - k_4x\right)}{r_2\cos\left(\frac{c_1k_4t}{d_1} - k_4x\right) + k_{10} + e^{-k_2t}}. \tag{27}$$

$$z(x,t) = \frac{2\left(\left(\kappa_3k_6^2\cosh(k_6x) - \kappa_2k_4^2\cos\left(\frac{c_1k_4t}{d_1} - k_4x\right)\right)(\Delta) - (\Delta_1)^2\right)}{(\Delta)^2}, \tag{28}$$

where $\Delta = \kappa_2\cos\left(\frac{c_1k_4t}{d_1} - k_4x\right) - \frac{\kappa_2k_{10}}{r_2} + e^{-k_2t} + \kappa_3\cosh(k_6x)$, and $\Delta_1 = \kappa_2k_4\sin\left(\frac{c_1k_4t}{d_1} - k_4x\right) + \kappa_3k_6\sinh(k_6x)$.

Now we get some dynamical representation of our solutions (Figs. 11 and 12):

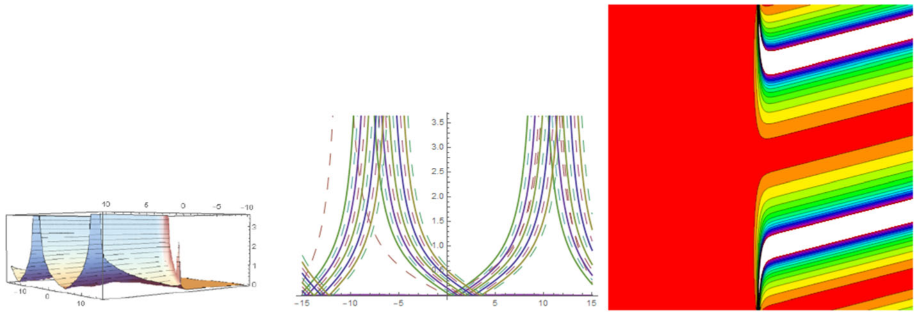

(a) (b) (c)

Fig. 11 *PCKS* graphical representation of solution $y(x, t)$ of Eq. (27) are shown as $k_2 = 5, k_4 = 0.2, k_{10} = 0.7 r_2 = 3, c_1 = 0.5, d_1 = 1.3, s = -2$.

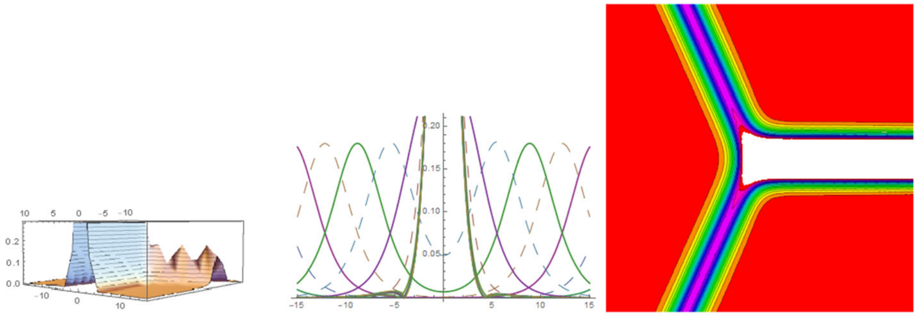

(a) (b) (c)

Fig. 12 *PCKS* graphical representation of solution $z(x, t)$ of Eq. (28) are shown as $k_2 = 2, k_4 = 0.2, k_6 = 0.6, k_{10} = 0.07, r_2 = 0.03, c_1 = 0.5, d_1 = 1.8, s = -5, \kappa_2 = 0.5, \kappa_3 = 4s$.

8 PCLWS

The *PCLWS*'s solution, which contains the sum of the quadratic functions and an exponential functions, is obtain in this section for Eq. (1). We use the following function g and j:

$$
\begin{aligned}
g &= \Lambda_1^2 + \Lambda_2^2 + n_1 \cos(H_1) + n_2 \cosh(H_2) + k_7, \\
j &= \Lambda_1^2 + \Lambda_2^2 + n_1 \cos(H_1) + n_2 \cosh(H_2) + k_8,
\end{aligned} \tag{29}
$$

Where

$$
\Lambda_1 = k_1 x + k_2 t + k_3, \quad \Lambda_2 = k_4 x + k_5 t + k_6, \quad H_1 = r_1 x + r_2 t, \quad H_2 = r_3 x + r_4 t,
$$

Put Eq. (25) into Eq. (4). We have values of the parameters which are given below:

$$
\begin{aligned}
& k_1 = k_1, k_2 = 0, k_3 = k_3, k_4 = k_4, k_5 = k_5, k_6 = k_6, k_7 = k_7, k_8 = 0, \\
& r_1 = 0, r_2 = r_2, r_3 = -\frac{d_1 r_4}{c_1}, r_4 = r_4,
\end{aligned} \tag{30}
$$

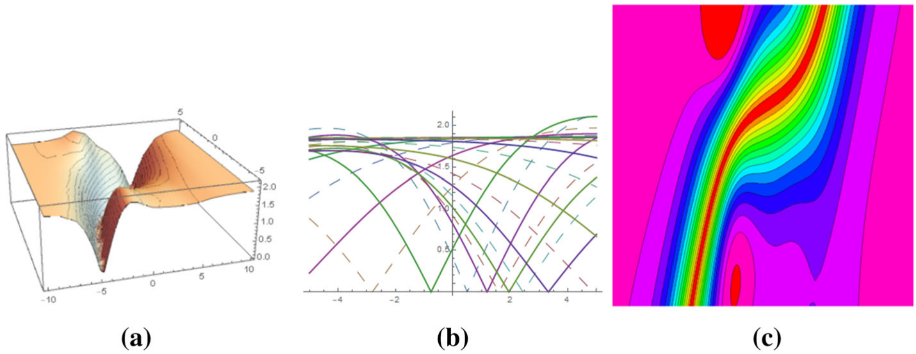

Fig. 13 *PCLWS* graphical representation of solution $y(x, t)$ of Eq. (31) are shown as $k_1 = 1.1, k_3 = 0.3, k_4 = -0.4, k_5 = 0.5,\ k_6 = 6.5, k_7 = 0.1, n_1 = 4.4, n_2 = 2.9, r_2 = 1.2, r_4 = 1.05, c_1 = 8.5, d_1 = 1.5, s = 5.$

Insert Eq. (30) into Eq. (29) and then in Eq. (3) to have the *PCLWS* solution of Eq. (1),

$$y(x,t) = \frac{2s\left(-\frac{d_1 n_2 r_4 \sinh\left(r_4 t - \frac{d_1 r_4 x}{c_1}\right)}{c_1} + 2k_1(k_1x + k_3) + 2k_4(k_4x + k_5t + \mathrm{k6})\right)}{n_2\cosh\left(r_4 t - \frac{d_1 r_4 x}{c_1}\right) + (k_1x + k_3)^2 + (k_4x + k_5t + k_6)^2 + k_7 + n_1\cos(r_2 t)}. \tag{31}$$

$$z(x,t) = \frac{2\left(\left(\Sigma + 2k_1^2 + 2k_4^2\right)(\Xi) - \left(-\Sigma + 2k_1(k_1x + k_3) + 2k_4(k_4x + k_5t + k_6)\right)^2\right)}{(\Xi)^2}, \tag{32}$$

where $\Xi = n_2\cosh\left(r_4 t - \frac{d_1 r_4 x}{c_1}\right) + (k_1x + k_3)^2 + (k_4x + k_5t + k_6)^2 + n_1\cos(r_2 t)$ and $\Sigma = \frac{d_1^2 n_2 r_4^2 \cosh\left(r_4 t - \frac{d_1 r_4 x}{c_1}\right)}{c_1^2}$.

Now we get some dynamical representation of our solutions (Figs. 13 and 14):

9 MWS

The *MWS*'s solution, which contains the sum of the quadratic functions and an exponential functions, is obtain in this section for Eq. (1). We use the following function g and j Seadawy et al. (2021):

$$\begin{aligned} g &= \kappa_0\cosh(\lambda_1) + \kappa_1\cos(\lambda_2) + \kappa_2\cosh(\lambda_3) + k_{10}, \\ j &= r_0\cosh(\lambda_1) + r_1\cos(\lambda_2) + r_2\cosh(\lambda_3) + k_{11}, \end{aligned} \tag{33}$$

Where

$$\lambda_1 = k_1x + k_2t + k_3, \quad \lambda_2 = k_4x + k_5t + k_6, \quad \lambda_3 = k_7x + k_8t + k_9,$$

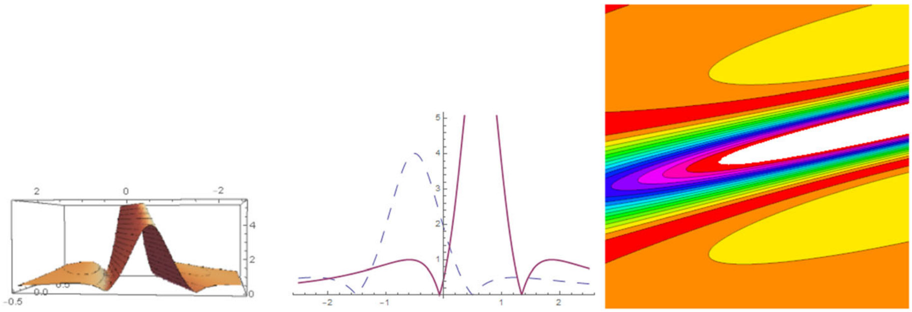

(a) **(b)** **(c)**

Fig. 14 *PCLWS* graphical representation of solution $z(x, t)$ of Eq. (32) are shown as $k_1 = -1, k_3 = 3.5, k_4 = 4, k_5 = -5, k_6 = 0.6, k_7 = -0.1, n_1 = -4.4, n_2 = 2.9, r_2 = -1.2, r_4 = 1, c_1 = -5, d_1 = 1.5, s = 5.$

Put Eq. (33) into Eq. (4). We have values of the parameters which are given below:

$$k_1 = 0, k_2 = 0, k_3 = 0, k_4 = k_4, k_5 = k_5, k_6 = 0, k_7 = 0, k_8 = 0, k_9 = k_9, k_{10} = k_{10},$$
$$k_{11} = 0, r_0 = 0, r_1 = -\frac{2\kappa_1 r_2\left(b_1 + 2c_1k_4^2 + 2d_1k_4k_5\right)}{\kappa_2\left(2b_1 + c_1k_4^2 + d_1k_4k_5\right)}, r_2 = r_2, \kappa_0 = \kappa_0, \kappa_1 = \kappa_1, \kappa_2 = \kappa_2 \tag{34}$$

Insert Eq. (34) into Eq. (33) and then in Eq. (3) to have the *MWS* solution of Eq. (1),

$$y(x,t) = -\frac{2\kappa_1 k_4 s \sin(k_4x + k_5t)}{\kappa_0 + k_{10} + \kappa_1\cos(k_4x + k_5t) + \kappa_2\cosh(k_9)}. \tag{35}$$

$$z(x,t) = \frac{2\left(\frac{2\kappa_1k_4^2r_2\left(b_1+2c_1k_4^2+2d_1k_4k_5\right)\cos(k_4x+k_5t)(\xi)}{\kappa_2\left(2b_1+c_1k_4^2+d_1k_4k_5\right)} - \frac{4\kappa_1^2k_4^2r_2^2\left(b_1+2c_1k_4^2+2d_1k_4k_5\right)^2\sin^2(k_4x+k_5t)}{\kappa_2^2\left(2b_1+c_1k_4^2+d_1k_4k_5\right)^2}\right)}{(\xi)^2}, \tag{36}$$

where $\xi = r_2\cosh(k_9) - \frac{2\kappa_1r_2\left(b_1+2c_1k_4^2+2d_1k_4k_5\right)\cos(k_4x+k_5t)}{\kappa_2\left(2b_1+c_1k_4^2+d_1k_4k_5\right)}$.

Now we get some dynamical representation of our solutions (Figs. 15 and 16):

10 LPKW

The *LPKW*'s solution, which contains the sum of the quadratic functions and an exponential functions, is obtain in this section for Eq. (1). We use the following function g and j Ren et al. (2019):

$$\begin{aligned} g &= \Lambda_1^2 + \Lambda_2^2 + n_1e^{H_1} + n_2\cos(\lambda) + k_7, \\ j &= \Lambda_1^2 + \Lambda_2^2 + n_1e^{H_1} + n_2\cos(\lambda)k_8, \end{aligned} \tag{37}$$

where

$$\Lambda_1 = k_1x + k_2t + k_3, \quad \Lambda_2 = k_4x + k_5t + k_6, \quad H_1 = r_1x + r_2t, \quad \lambda = m_1x + m_2t,$$

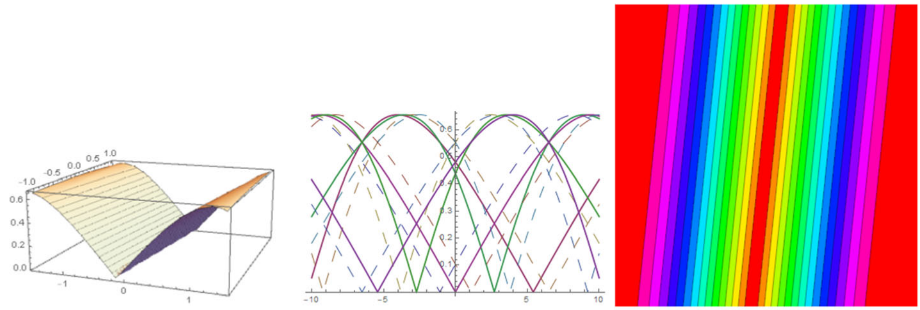

(a) (b) (c)

Fig. 15 *MWS* graphical representation of solution $y(x, t)$ of Eq. (35) are shown as $k_4 = -0.2, k_5 = 1.3, k_9 = 0.05, k_{10} = 0.1, s = 5, \kappa_0 = 2.5, \kappa_1 = 1.9, \kappa_2 = 3.5$.

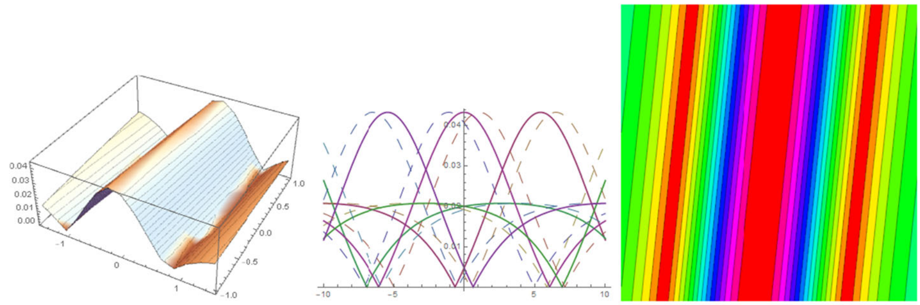

(a) (b) (c)

Fig. 16 *MWS* graphical representation of solution $z(x, t)$ of Eq. (36) are shown as $k_4 = -0.2, k_5 = 1.5, k_9 = 0.05, k_{10} = 0.1, s = 5, \kappa_0 = 2.5, \kappa_1 = 1.9, \kappa_2 = 3.5, b_1 = 5, d_1 = 4.5, c_1 = 3, r_2 = 2$.

Put Eq. (37) into Eq. (4). We have values of the parameters which are given below:

$$k_1 = 0, k_2 = 0, k_3 = k_3, k_4 = k_4, k_5 = k_5, k_6 = 0, k_7 = \frac{1}{3}(-2)k_3^2, k_8 = 0, \tag{38}$$

Insert Eq. (38) into Eq. (37) and then in Eq. (3) to have the *LPKW* solution of Eq. (1),

$$y(x,t) = \frac{2s(2k_4(k_4x + k_5t) - m_1n_2\sin(m_1x + m_2t) + \mathrm{n1}r_1e^{r_1x+r_2t})}{\frac{k_3^2}{3} + (k_4x + k_5t)^2 + n_2\cos(m_1x + m_2t) + n_1e^{r_1x+r_2t}}. \tag{39}$$

$$z(x,t) = \frac{2\left(\left(2k_4^2 - m_1^2n_2\cos(\theta) + n_1r_1^2e^{r_1x+r_2t}\right)(\varrho) - \left(2k_4(k_4x + k_5t) - m_1n_2\sin(\theta) + n_1r_1e^{r_1x+r_2t}\right)^2\right)}{(\varrho)^2}, \tag{40}$$

where $\theta = m_1x + m_2t$ and $\varrho = k_3^2 + (k_4x + k_5t)^2 + n_2\cos(\theta) + n_1e^{r_1x+r_2t}$.

Now we get some dynamical representation of our solutions (Figs. 17 and 18):

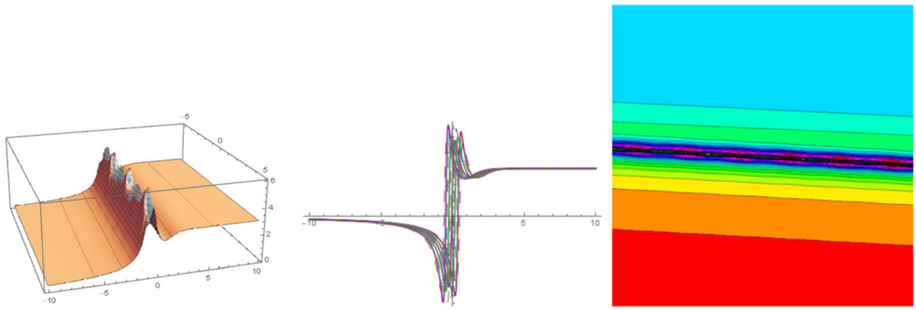

(a) (b) (c)

Fig. 17 *LPKW* graphical representation of solution $y(x, t)$ of Eq. (39) are shown as $k_3 = -0.9, k_4 = 10, k_5 = 1.1, s = 0.5, r_1 = 3, r_2 = 0.3, n_1 = 5, n_2 = 0.8, m_1 = 2.5, m_2 = 4$.

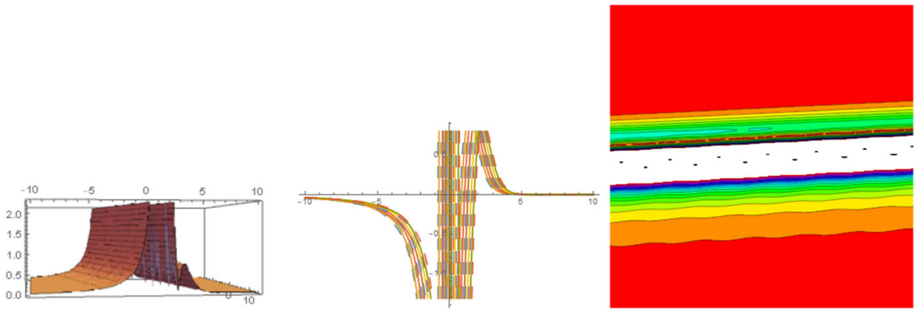

(a) (b) (c)

Fig. 18 *LPKW* graphical representation of solution $z(x, t)$ of Eq. (40) are shown as $k_3 = -0.9, k_4 = 10, k_5 = -1.1, s = 0.5, r_1 = 3, r_2 = -0.3, n_1 = 5, n_2 = -0.8, m_1 = 2.5, m_2 = -4$.

11 BLWS

The *BLWS*'s solution, which contains the sum of the quadratic functions and an exponential functions, is obtain in this section for Eq. (1). We use the following function g and j Seadawy et al. (2021):

$$\begin{aligned} g &= e^{-h\Lambda_1} + m_1 e^{h\Lambda_1} + n_2 \cos(h_1\Lambda_2) + k_6, \\ j &= e^{-h\Lambda_1} + n_1 e^{h\Lambda_1} + n_2 \cos(h_1\Lambda_2) + k_7, \end{aligned} \tag{41}$$

where

$$\Lambda_1 = k_1 x + k_2 t + k_3, \quad \Lambda_2 = k_4 x + k_5 t,$$

Put Eq. (41) into Eq. (4). We have values of the parameters which are given below:

$$k_1 = 0, k_2 = k_2, k_3 = k_3, k_4 = -\frac{d_1 k_5}{c_1}, k_5 = k_5, k_6 = k_6, n_1 = n_1, n_2 = n_2 \tag{42}$$

Insert Eq. (42) into Eq. (41) and then in Eq. (3) to have the *BLWS* solution of Eq. (1),

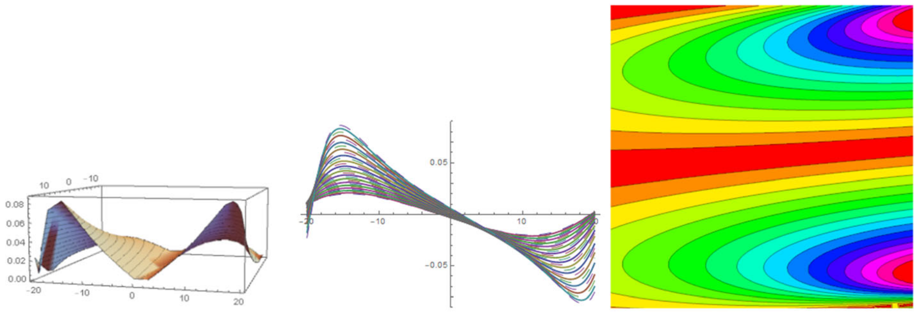

(a) (b) (c)

Fig. 19 *BLWS* graphical representation of solution $y(x, t)$ of Eq. (43) are shown as $k_2 = -0.5, k_3 = 7, k_5 = 0.05, k_6 = 0.7, s = 0.2, d_1 = 5, h = 0.1, h_1 = 0.3, n_1 = 2, n_2 = 3, c_1 = 0.5.$

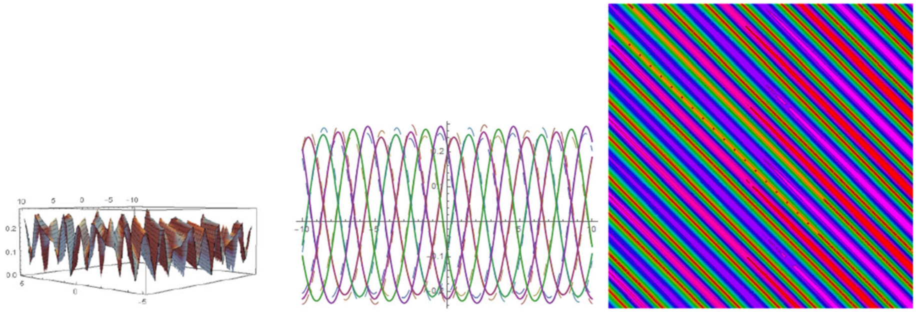

(a) (b) (c)

Fig. 20 *BLWS* graphical representation of solution $z(x, t)$ of Eq. (44) are shown as $k_2 = 0.7, k_3 = 0.7, k_5 = 5, k_6 = 7, k_7 = -0.8,\ s = 0.5, d_1 = -3, h = 0.01, h_1 = 0.5, n_1 = 0.2, n_2 = 0.03, c_1 = 6.$

$$y(x,t) = \frac{2 d_1 h_1 k_5 n_2 s \sin\left(h_1\left(k_5 t - \frac{d_1 k_5 x}{\mathrm{c1}}\right)\right)}{c_1\left(n_2 \cos\left(h_1\left(k_5 t - \frac{d_1 k_5 x}{c_1}\right)\right) + n_1 e^{h(k_2 t + k_3)} + e^{-h(k_2 t + k_3)} + k_6\right)}. \tag{43}$$

$$z(x,t) = \frac{2\left(-\frac{d_1^2 h_1^2 k_5^2 n_2 \cos(\varphi)\left(n_2 \cos(\varphi) + n_1 e^{h(k_2 t + k_3)} + e^{-h(k_2 t + k_3)} + \mathrm{k7}\right)}{c_1^2} - \frac{d_1^2 h_1^2 k_5^2 n_2^2 \sin^2(\varphi)}{c_1^2}\right)}{\left(n_2 \cos(\varphi) + n_1 e^{h(k_2 t + k_3)} + e^{-h(k_2 t + k_3)} + k_7\right)^2}, \tag{44}$$

where $\varphi = h_1\left(k_5 t - \frac{d_1 k_5 x}{c_1}\right)$.

Now we get some dynamical representation of our solutions (Figs. 19 and 20):

12 Traveling wave transformation (TWT)

To solve Eqs. (1) and (2), the *TWT* are formed as Biswas et al. (2022),

$$y(x,t) = Y_1(v)e^{i\xi_1(x,t)}, \tag{45}$$

$$z(x,t) = Y_2(v)e^{2i\xi_2(x,t)}. \tag{46}$$

$Y_j(v)$ for j=1,2 are components of amplitude and wave variables is

$$v = \psi(x - qt), \tag{47}$$

where ψ and q are the real-valued constants that symbolize the soliton width and velocity, and the phase components are given as

$$\xi_j(x,t) = -px + vt + \phi, \tag{48}$$

where p, v and ϕ are the real-valued constants that represents the soliton frequency, soliton wave number and phase constant respectively.

Next By putting Eqs. (45) and (46) in Eqs. (1) and (2) we have the real and imaginary parts are

$$\psi^2(c_1 - qd_1)Y_1^{''} + (b_1 - v - p^2c_1 + pvd_1 - pa_1)Y_1 + \alpha_1 Y_1 Y_2 = 0, \tag{49}$$

$$pqd_1 - 2pc_1 + vd_1 - q - a_1 = 0, \tag{50}$$

$$\psi^2(c_2 - qd_2)Y_2^{''} + (b_2 - 2v - 4p^2c_2 + 4pvd_2 - 2pa_2)Y_2 + \alpha_2 Y_1^2 = 0, \tag{51}$$

$$2pqd_2 - 4pc_2 + 2vd_2 - q - a_2 = 0, \tag{52}$$

Equations (49)–(52) shorten to ordinary differential equation by using balancing rule

$$\psi^2(c - qd)Y^{''} + (2cp^2 - 2dpv + ap + v)Y + \alpha Y^2 = 0, \tag{53}$$

with velocity

$$q = \frac{4pc - 2vd + \eta}{2pd - 1}, \tag{54}$$

and constraints are

$$\begin{aligned} &Y_1 = Y_2 = Y, d_1 = 2d, d_2 = d, c_1 = 2c, c_2 = c, a_1 = a_2 = a, \\ &\alpha_1 = 2\alpha, \alpha_2 = \alpha, b_1 = b_2 = b, b = 6cp^2 - 6dpv + 3ap + 3v. \end{aligned} \tag{55}$$

Now we apply the transformation below for variety of rational solutions

$$Y = 2(logg)_\zeta, \tag{56}$$

Eq. (56) is inserted into Eq. (51) to generate the following bilinear form,

$$4cdp\psi^2g^2g''' + 2c\psi^2g^2g''' - 4d^2v\psi^2g^2g''' + 2d\eta\psi^2g^2g''' - 4adp^2g^2g' + 2apg^2g' - 8cdp^3g^2g' + 8cdp\psi^2g'^3 - 12cdp\psi^2gg'g'' + 4c\psi^2g'^3 + 4cp^2g^2g' - 6c\psi^2gg'g'' + 8d^2p^2vg^2g' - 8d^2v\psi^2g'^3 + 12d^2v\psi^2gg'g'' + 4d\eta\psi^2g'^3 - 8\alpha dpgg'^2 - 8dpvg^2g' - 6d\eta\psi^2gg'g'' + 4\alpha gg'^2 + 2vg^2g' \tag{57}$$

The remaining part of the paper is structured as following:

13 MSRS

For solving *MSRS* we use the following transformation (Ashraf et al. 2022),

$$\begin{aligned} &g = \sigma_1^2 + \sigma_2^2 + u_5, \\ &\sigma_1 = u_1\zeta + u_2, \quad \sigma_2 = u_3\zeta + u_4, \end{aligned} \tag{58}$$

inserting Eq. (58) into Eq. (57) and we have some values of parameters

$$\begin{aligned} u_1 &= \frac{i\left(u_4^2 + u_5\right)(ap + 2cp^2 - 2dpv + v)}{2(\alpha u_4)}, \\ u_3 &= -\frac{apu_4^2 + apu_5 + 2cp^2u_4^2 + 2cp^2u_5 - 2dpu_4^2v - 2dpu_5v + u_4^2v + u_5v}{2(\alpha u_4)}, \\ u_2 &= 0, u_4 = u_4, u_5 = u_5, \end{aligned} \tag{59}$$

For *MSRS* of Eqs. (45) and (46) substitute Eq. (59) into Eq. (58) and then put in Eq. (56),

$$y_1(x,t) = \frac{2e^{i(-px+vt+\phi)}\left(-\frac{\psi\beta(\gamma)}{2\alpha^2u_4^2} - \frac{(\delta)(\varpi)}{\alpha u_4}\right)}{-\frac{\psi^2\beta(\gamma)^2}{4\alpha^2u_4^2} + (\varpi)^2 + u_5}, \tag{60}$$

$$z_1(x,t) = \frac{2e^{2i(-px+vt+\phi)}\left(-\frac{\psi\beta\tau}{2\alpha^2u_4^2} - \frac{(\delta)(\varpi)}{\alpha u_4}\right)}{-\frac{\psi^2\beta(\tau)^2}{4\alpha^2u_4^2} + (\varpi)^2 + u_5}, \tag{61}$$

where $\beta = \left(u_4^2 + u_5\right)^2(ap + 2cp^2 - 2dpv + v)^2$, $\gamma = x - \frac{t(4cp-2dv+\eta)}{2dp-1}$, $\delta = apu_4^2 + apu_5 + 2cp^2u_4^2 + 2cp^2u_5 - 2dpu_4^2v - 2dpu_5v + u_4^2v + u_5v$, $\tau = x - \frac{t(4cp-2dv+\eta)}{2dp-1}$ and $\varpi = u_4 - \frac{\psi(\delta)\tau}{2\alpha u_4}$.

14 MSR1K

For solving *MSR1K* we use the following transformation (Ashraf et al. 2022),

$$\begin{aligned} &g = \sigma_1^2 + \sigma_2^2 + z_1e^{V_1} + u_5, \\ &\sigma_1 = u_1\zeta + u_2, \quad \sigma_2 = u_3\zeta + u_4, \\ &V_1 = w_1\zeta + w_2, \end{aligned} \tag{62}$$

inserting Eq. (62) into Eq. (57) and we have some values of parameters

$$u_1 = 0, u_2 = u_2, u_3 = -\frac{3u_4(ap + 2cp^2 - 2dpv + v)}{2\alpha},$$
$$u_4 = u_4, u_5 = u_5, w_1 = 0, w_2 = w_2, z_1 = z_1, \tag{63}$$

For *MSR*1*K* of Eqs. (45) and (46) substitute Eq. (63) into Eq. (62) and then put in Eq. (56),

$$y_2(x,t) = -\frac{6u_4 e^{i(-px+vt+\phi)}(ap + 2cp^2 - 2dpv + v)\left(u_4 - \frac{3u_4\psi\left(ap+2cp^2-2dpv+v\right)\left(x-\frac{t(4cp-2dv+\eta)}{2dp-1}\right)}{2\alpha}\right)}{\alpha\left(\left(u_4 - \frac{3u_4\psi(ap+2cp^2-2dpv+v)\left(x-\frac{t(4cp-2dv+\eta)}{2dp-1}\right)}{2\alpha}\right)^2 + u_2^2 + u_5 + e^{w_2}z_1\right)}. \tag{64}$$

$$z_2(x,t) = -\frac{6u_4 e^{2i(-px+vt+\phi)}(ap + 2cp^2 - 2dpv + v)\left(u_4 - \frac{3u_4\psi\left(ap+2cp^2-2dpv+v\right)\left(x-\frac{t(4cp-2dv+\eta)}{2dp-1}\right)}{2\alpha}\right)}{\alpha\left(\left(u_4 - \frac{3u_4\psi(ap+2cp^2-2dpv+v)\left(x-\frac{t(4cp-2dv+\eta)}{2dp-1}\right)}{2\alpha}\right)^2 + u_2^2 + u_5 + e^{w_2}z_1\right)}. \tag{65}$$

15 MSR2K

For solving *MSR*2*K* we use the following transformation (Ashraf et al. 2022),

$$g = \sigma_1^2 + \sigma_2^2 + r_1 e^{V_1} + z_2 e^{V_2} + u_5,$$
$$\sigma_1 = u_1\zeta + u_2, \quad \sigma_2 = u_3\zeta + u_4, \tag{66}$$
$$V_1 = w_1\zeta + w_2, \quad V_2 = w_3\zeta + u_4,$$

inserting Eq. (66) into Eq. (57) and we have some values of parameters

$$u_1 = 0, u_2 = u_2, u_3 = -\frac{3u_4(ap + 2cp^2 - 2dpv + v)}{2\alpha},$$
$$u_4 = u_4, u_5 = u_5, w_1 = w_1, w_2 = w_2, w_3 = 0, w_4 = w_4, z_1 = z_1, z_2 = z_2, \tag{67}$$

For *MSR*2*K* of Eqs. (45) and (46) substitute Eq. (66) into Eq. (67) and then put in Eq. (56),

$$y_3(x,t) = \frac{2e^{i(-px+vt+\phi)}\left(w_1 z_1 e^{\left(w_1\psi\left(x-\frac{t(4cp-2dv+\eta)}{2dp-1}\right)+w_2\right)} - \frac{3u_4\left(ap+2cp^2-2dpv+v\right)(\varepsilon)}{\alpha}\right)}{(\varepsilon)^2 + z_1 e^{\left(w_1\psi\left(x-\frac{t(4cp-2dv+\eta)}{2dp-1}\right)+w_2\right)} + u_2^2 + u_5 + e^{w_4}z_2}, \tag{68}$$

$$z_3(x,t) = \frac{2e^{2i(-px+vt+\phi)}\left(w_1 z_1 e^{\left(w_1\psi\left(x-\frac{t(4cp-2dv+\eta)}{2dp-1}\right)+w_2\right)} - \frac{3u_4\left(ap+2cp^2-2dpv+v\right)(\varepsilon)}{\alpha}\right)}{(\varepsilon)^2 + z_1 e^{\left(w_1\psi\left(x-\frac{t(4cp-2dv+\eta)}{2dp-1}\right)+w_2\right)} + u_2^2 + u_5 + e^{w_4}z_2}, \tag{69}$$

where $\varepsilon = u_4 - \frac{3u_4\psi\left(ap+2cp^2-2dpv+v\right)\left(x-\frac{t(4cp-2dv+\eta)}{2dp-1}\right)}{2\alpha}$.

16 HBS

For solving *HBS* we use the following transformation (Ahmed et al. 2019b),

$$g = e^{-u(w_1\zeta+w_2)} + z_1 e^{w(u_3\zeta+u_4)} + z_2 \cos(u_1(w_5\zeta + w_6)), \tag{70}$$

inserting Eq. (70) into Eq. (57) and we have some values of parameters

$$u = \frac{ap + 2cp^2 - 2dpv + v}{2(mw_1)}, u_1 = u_1, w_1 = w_1, w_2 = w_2, w_3 = 0, w_4 = w_4, w_5 = w_5, w_6 = w_6, \\ z_1 = 0, z_2 = 0, \tag{71}$$

For *HBS* of Eqs. (45) and (46) substitute Eq. (71) into Eq. (70) and then put in Eq. (56),

$$y_4(x,t) = -\frac{e^{i(-px+vt+\phi)}(ap + 2cp^2 - 2dpv + v)}{\alpha}. \tag{72}$$

$$z_4(x,t) = -\frac{e^{2i(-px+vt+\phi)}(ap + 2cp^2 - 2dpv + v)}{\alpha}. \tag{73}$$

17 PCRS

For solving *PCRS* we use the following transformation (Ahmed et al. 2019a),

$$\begin{aligned} &g = \sigma_1^2 + \sigma_2^2 + z_1 \cos(V_1) + z_2 \cosh(V_2) + u_5, \\ &\sigma_1 = u_1\zeta + u_2, \quad \sigma_2 = u_3\zeta + u_4, \\ &V_1 = w_1\zeta + w_2, \quad V_2 = w_3\zeta + w_4, \end{aligned} \tag{74}$$

inserting Eq. (74) into Eq. (57) and we have some values of parameters:

$$u_1 = 0, u_2 = u_2, u_3 = u_3, u_4 = \frac{3\left(\psi^2 u_3(2cdp + c - 2d^2v + d\eta)\right)}{4(\alpha(2dp - 1))}, u_5 = u_5, z_1 = 0, z_2 = 0, \\ w_1 = w_1, w_2 = w_2, w_3 = \frac{\sqrt{-\frac{-2adp^2+ap-4cdp^3+2cp^2+4d^2p^2v-4dpv+v}{2cdp+c-2d^2v+d\eta}}}{\psi}, \tag{75}$$

For *PCRS* of Eqs. (45) and (46) substitute Eq. (75) into Eq. (74) and then put in Eq. (56),

$$y_5(x,t) = \frac{2e^{i(-px+vt+\phi)}\left(\frac{z_2\sqrt{\frac{2adp^2-ap+4cdp^3-2cp^2-4d^2p^2v+4dpv-v}{2cdp+c-2d^2v+d\eta}}\sinh(\theta)}{\psi} + 2u_3(\rho) - w_1 z_1 \sin(\Omega)\right)}{z_2\cosh(\theta) + (\rho)^2 + z_1\cos(\Omega) + u_2^2 + u_5}, \tag{76}$$

$$z_5(x,t)=\frac{2e^{2i(-px+vt+\phi)}\left(\frac{z_2\sqrt{\frac{2adp^2-ap+4cdp^3-2cp^2-4d^2p^2v+4dpv-v}{2cdp+c-2d^2v+d\eta}}\sinh(\theta)}{\psi}+2u_3(\rho)-w_1z_1\sin(\Omega)\right)}{z_2\cosh(\theta)+(\rho)^2+z_1\cos(\Omega)+u_2^2+u_5}, \tag{77}$$

where $\theta=\sqrt{\frac{2adp^2-ap+4cdp^3-2cp^2-4d^2p^2v+4dpv-v}{2cdp+c-2d^2v+d\eta}}\left(x-\frac{t(4cp-2dv+\eta)}{2dp-1}\right)+w_4$ and $\rho=\frac{3u_3\psi^2\left(2cdp+c-2d^2v+d\eta\right)}{4\alpha(2dp-1)}+u_3\psi\left(x-\frac{t(4cp-2dv+\eta)}{2dp-1}\right)$ and $\Omega=w_1\psi\left(x-\frac{t(4cp-2dv+\eta)}{2dp-1}\right)+w_2$.

18 KCRS

For solving *KCRS* we use the following transformation (Ahmed et al. 2019a, b),

$$\begin{aligned}&g=e^{-V_1}+z_1e^{V_1}+\sigma_1^2+\sigma_2^2+u_5,\\&\sigma_1=u_1\zeta+u_2,\quad \sigma_2=u_3\zeta+u_4,\\&V_1=w_1\zeta+w_2,\end{aligned} \tag{78}$$

inserting Eq. (78) into Eq. (57) and we have some values of parameters

$$\begin{aligned}&u_1=0,u_2=u_2,u_3=-\frac{3u_4(ap+2cp^2-2dpv+v)}{2\alpha},u_4=u_4,u_5=u_5,z_1=z_1\\&w_1=0,w_2=w_2,\end{aligned} \tag{79}$$

For *KCRS* of Eqs. (45) and (46) substitute Eq. (79) into Eq. (78) and then put in Eq. (56),

$$y_6(x,t)=-\frac{6u_4e^{i(-px+vt+\phi)}(ap+2cp^2-2dpv+v)\left(u_4-\frac{3u_4\psi\left(ap+2cp^2-2dpv+v\right)\left(x-\frac{t(4cp-2dv+\eta)}{2dp-1}\right)}{2\alpha}\right)}{\alpha\left(\left(u_4-\frac{3u_4\psi(ap+2cp^2-2dpv+v)\left(x-\frac{t(4cp-2dv+\eta)}{2dp-1}\right)}{2\alpha}\right)^2+u+u_2^2+e^{w_2}z_1+e^{-w_2}\right)}. \tag{80}$$

$$z_6(x,t)=-\frac{6u_4e^{2i(-px+vt+\phi)}(ap+2cp^2-2dpv+v)\left(u_4-\frac{3u_4\psi\left(ap+2cp^2-2dpv+v\right)\left(x-\frac{t(4cp-2dv+\eta)}{2dp-1}\right)}{2\alpha}\right)}{\alpha\left(\left(u_4-\frac{3u_4\psi(ap+2cp^2-2dpv+v)\left(x-\frac{t(4cp-2dv+\eta)}{2dp-1}\right)}{2\alpha}\right)^2+u+u_2^2+e^{w_2}z_1+e^{-w_2}\right)}. \tag{81}$$

19 MSPK

For solving *MSPK* we use the following transformation (Ahmed et al. 2019b),

$$\begin{aligned} &g = \sigma_1^2 + \sigma_2^2 + +z_1\cos(V_1) + z_2 e^{V_2} + u_5, \\ &\sigma_1 = u_1\zeta + u_2, \quad \sigma_2 = u_3\zeta + u_4, \\ &V_1 = w_1\zeta + w_2, \quad V_2 = w_3\zeta + w_4, \end{aligned} \tag{82}$$

inserting Eq. (82) into Eq. (57) and we have some values of parameters:

$$\begin{aligned} &u_1 = 0, u_2 = u_2, u_3 = u_3, u_4 = \frac{3\psi^2 u_3(2cdp + c - 2d^2v + d\eta)}{4(\alpha(2dp-1))}, u_5 = u_5, \\ &w_1 = \frac{\sqrt{-\frac{2adp^2 - ap + 4cdp^3 - 2cp^2 - 4d^2p^2v + 4dpv - v}{2cdp + c - 2d^2v + d\eta}}}{\psi}, w_3 = w_3, w_4 = w_4, w_2 = w_2 z_1 = z_1, z_2 = z_2, \end{aligned} \tag{83}$$

For *MSPK* of Eqs. (45) and (46) substitute Eq. (83) into Eq. (82) and then put in Eq. (56),

$$y_7(x,t) = \frac{2e^{i(-px+vt+\phi)}\left(\Gamma + 2u_3\left(\frac{3u_3\psi^2\left(2cdp+c-2d^2v+d\eta\right)}{4\alpha(2dp-1)} + u_3\psi\left(x - \frac{t(4cp-2dv+\eta)}{2dp-1}\right)\right) + w_3 z_2 e^{\Theta}\right)}{z_1\cos(\xi) + \left(\frac{3u_3\psi^2(2cdp+c-2d^2v+d\eta)}{4\alpha(2dp-1)} + u_3\psi\left(x - \frac{t(4cp-2dv+\eta)}{2dp-1}\right)\right)^2 + z_2 e^{\Theta} + u_2^2 + u_5}, \tag{84}$$

$$z_7(x,t) = \frac{2e^{2i(-px+vt+\phi)}\left(\Gamma + 2u_3\left(\frac{3u_3\psi^2\left(2cdp+c-2d^2v+d\eta\right)}{4\alpha(2dp-1)} + u_3\psi\left(x - \frac{t(4cp-2dv+\eta)}{2dp-1}\right)\right) + w_3 z_2 e^{\Theta}\right)}{z_1\cos(\xi) + \left(\frac{3u_3\psi^2(2cdp+c-2d^2v+d\eta)}{4\alpha(2dp-1)} + u_3\psi\left(x - \frac{t(4cp-2dv+\eta)}{2dp-1}\right)\right)^2 + z_2 e^{\Theta} + u_2^2 + u_5}, \tag{85}$$

where $\xi = \sqrt{\frac{-2adp^2 + ap - 4cdp^3 + 2cp^2 + 4d^2p^2v - 4dpv + v}{2cdp + c - 2d^2v + d\eta}}\left(x - \frac{t(4cp-2dv+\eta)}{2dp-1}\right) + w_2$ and $\Gamma = -\frac{z_1\sqrt{\frac{-2adp^2 + ap - 4cdp^3 + 2cp^2 + 4d^2p^2v - 4dpv + v}{2cdp + c - 2d^2v + d\eta}}\sin(\xi)}{\psi}$ and $\Theta = w_3\psi\left(x - \frac{t(4cp-2dv+\eta)}{2dp-1}\right) + w_4 + u_2^2 + u_5$.

20 MSRK

For solving *MSRK* we use the following transformation (Seadawy et al. 2021; Manafian et al. 2020),

$$\begin{aligned} &g = \sigma_1^2 + \sigma_2^2 + +z_1\cosh(V_1) + z_2 e^{V_2} + u_5, \\ &\sigma_1 = u_1\zeta + u_2, \quad \sigma_2 = u_3\zeta + u_4, \\ &V_1 = w_1\zeta + w_2, \quad V_2 = w_3\zeta + w_4, \end{aligned} \tag{86}$$

inserting Eq. (86) into Eq. (57) and we have some values of parameters:

$$u_1 = 0, u_2 = u_2, u_3 = u_3, u_4 = \frac{3\left(\psi^2 u_3 (2cdp + c - 2d^2 v + d\eta)\right)}{4(\alpha(2dp-1))}, u_5 = u_5,$$
$$w_1 = \frac{\sqrt{-\frac{-2adp^2+ap-4cdp^3+2cp^2+4d^2p^2v-4dpv+v}{2cdp+c-2d^2v+d\eta}}}{\psi}, w_3 = w_3, w_4 = w_4, w_2 = w_2 z_1 = z_1, z_2 = z_2, \tag{87}$$

For *MSRK* of Eqs. (45) and (46) insert Eq. (87) into Eq. (86) and then put in Eq. (56),

$$y_8(x,t) = \frac{2e^{i(-px+vt+\phi)}\left(\frac{z_1\sqrt{\frac{2adp^2-ap+4cdp^3-2cp^2-4d^2p^2v+4dpv-v}{2cdp+c-2d^2v+d\eta}}\sinh(\Phi)}{\psi} + 2u_3(\Delta) + w_3 z_2 e^{\omega}\right)}{z_1\cosh(\Phi) + (\Delta)^2 + z_2 e^{\omega} + u_2^2 + u_5}, \tag{88}$$

$$z_8(x,t) = \frac{2e^{2i(-px+vt+\phi)}\left(\frac{z_1\sqrt{\frac{2adp^2-ap+4cdp^3-2cp^2-4d^2p^2v+4dpv-v}{2cdp+c-2d^2v+d\eta}}\sinh(\Phi)}{\psi} + 2u_3(\Delta) + w_3 z_2 e^{\omega}\right)}{z_1\cosh(\Phi) + (\Delta)^2 + z_2 e^{\omega} + u_2^2 + u_5}, \tag{89}$$

where $\Phi = \sqrt{\frac{2adp^2-ap+4cdp^3-2cp^2-4d^2p^2v+4dpv-v}{2cdp+c-2d^2v+d\eta}}\left(x - \frac{t(4cp-2dv+\eta)}{2dp-1}\right) + w_2,$ $\Delta = \frac{3u_3\psi^2\left(2cdp+c-2d^2v+d\eta\right)}{4\alpha(2dp-1)} + u_3\psi\left(x - \frac{t(4cp-2dv+\eta)}{2dp-1}\right)$ and $\omega = w_3\psi\left(x - \frac{t(4cp-2dv+\eta)}{2dp-1}\right) + w_4.$

21 Stability

Now using Hamiltonian method Γ framework, we examine the stability (Khater 2019),

$$\Gamma_1 = \frac{1}{2}\int_{-p}^{p} y^2(x)dx \quad \Gamma_2 = \frac{1}{2}\int_{-p}^{p} z^2(x)dx, \tag{90}$$

Now we verify the stability as

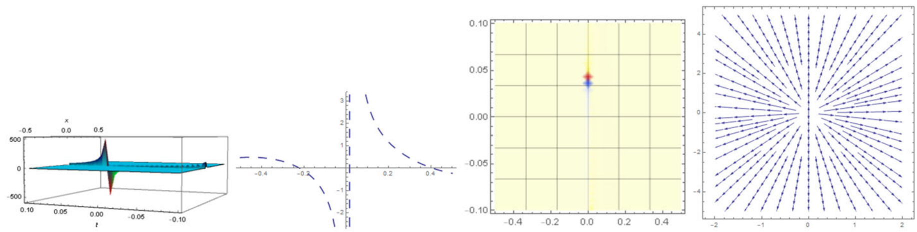

(a) (b) (c) (d)

Fig. 21 Graphical representation of solution $y_1(x,t)$ in Eq. (60) are presented via $a = 2, \alpha = 0.8, c = 0.01, d = -4, \eta = 2, p = 5,$ $u = 2, u_2 = 0.06, u_3 = -0.03, u_4 = -0.9, u_5 = 5, v = 0.3, w_2 = 5, w_3 = 3, w_4 = -7,$ $\psi = 8, z_1 = 0.9, z_2 = -5, \phi = 0.5,$ (a) 3D plot (b) 2D plot (c) density plot and (d) stream plot respectively

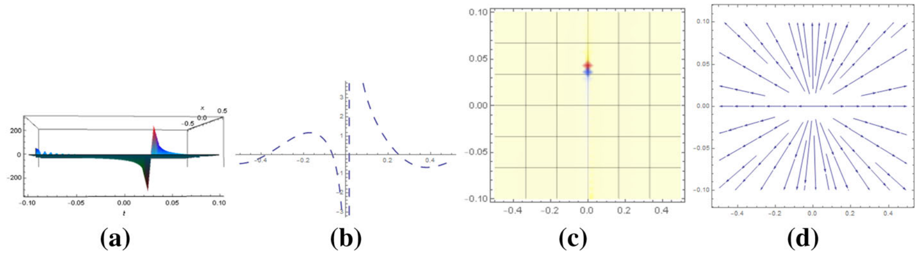

Fig. 22 Graphical representation of solution $z_1(x,t)$ in Eq. (61) are presented via $a = 2, \alpha = 0.8, c = 0.01, d = -4, \eta = 2, p = 5, u = 2, u_2 = 0.06, u_3 = -0.03, u_4 = -0.9, u_5 = 5, v = 0.3, w_2 = 5, w_3 = 3, w_4 = -7, \psi = 8, z_1 = 0.9, z_2 = -5, \phi = 0.5$

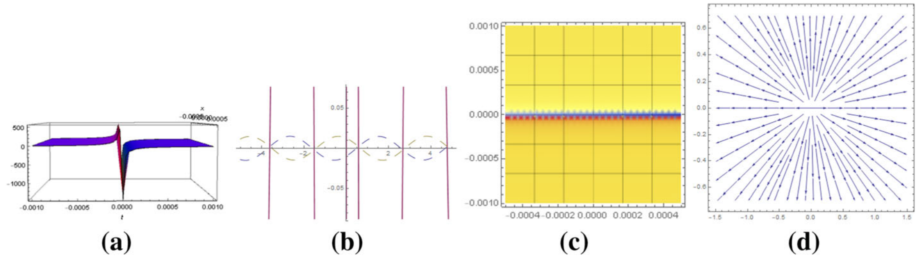

Fig. 23 Graphical representation of solution $y_2(x,t)$ in Eq. (64) are presented via $a = -2, \alpha = -0.2, c = 10, d = 0.4, \eta = 5, \quad p = 1.5, u = -2, u_2 = 0.6, u_3 = -3, u_4 = 1.9, u_5 = -0.5, v = -3, w_2 = 1.5, w_3 = 0.03, w_4 = -0.7, \psi = -0.8, z_1 = -0.1, z_2 = 5, \phi = 15$

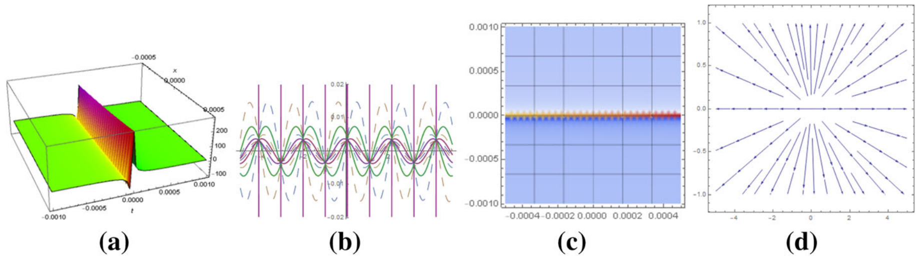

Fig. 24 Graphical representation of solution $z_2(x,t)$ in Eq. (65) are presented via $a = -2, \alpha = -0.2, c = 10, d = 0.4, \eta = 5, p = 1.5, \quad u = -2, u_2 = 0.6, u_3 = -3, u_4 = 1.9, u_5 = -0.5, v = -3, w_2 = 1.5, w_3 = 0.03, w_4 = -0.7, \psi = -0.8, z_1 = -0.1, z_2 = 5, \phi = 15$

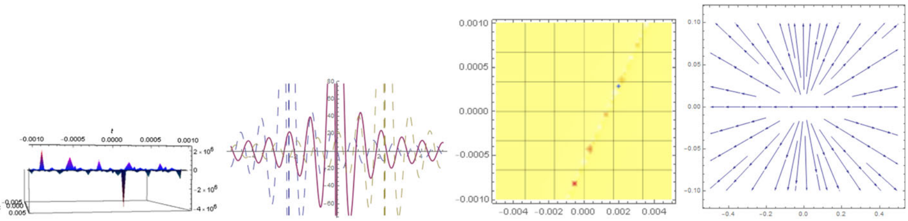

(a) **(b)** **(c)** **(d)**

Fig. 25 Graphical representation of solution $y_3(x,t)$ in Eq. (68) are presented via $a=-2.4, \alpha=-0.2, c=1.7, d=2.4, \eta=5.5, p=6.5, u=2.5, u_2=-0.6, u_3=-0.03, u_4=-1.9, u_5=0.5, v=-3.9, w_1=0.4, w_2=1.05, w_3=3.7, w_4=0.7, \psi=0.08, z_1=0.01, z_2=-3, \phi=1.05$

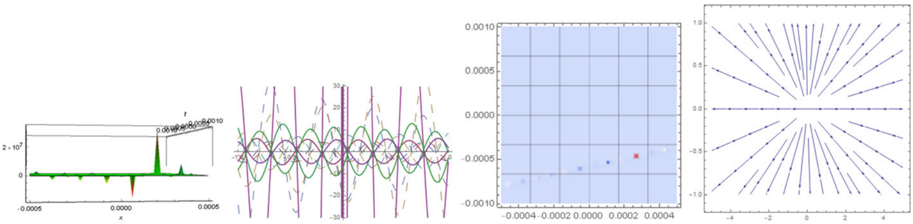

(a) **(b)** **(c)** **(d)**

Fig. 26 Graphical representation of solution $z_3(x,t)$ in Eq. (69) are presented via $a=-2.4, \alpha=-0.2, c=1.7, d=2.4, \eta=5.5, p=6.5, u=2.5, u_2=-0.6, u_3=-0.03, u_4=-1.9, u_5=0.5, v=-3.9, w_1=0.4, w_2=1.05, w_3=3.7, w_4=0.7, \psi=0.08, z_1=0.01, z_2=-3, \phi=1.05$

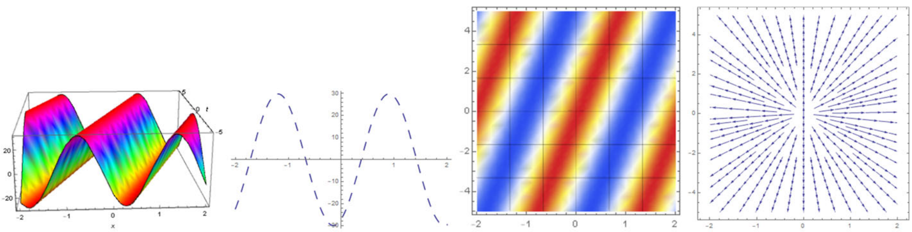

(a) **(b)** **(c)** **(d)**

Fig. 27 Graphical representation of solution $y_4(x,t)$ in Eq. (72) are presented via $a=5, \alpha=-0.5, c=0.3, d=2, p=3, v=0.5, \phi=0.2$

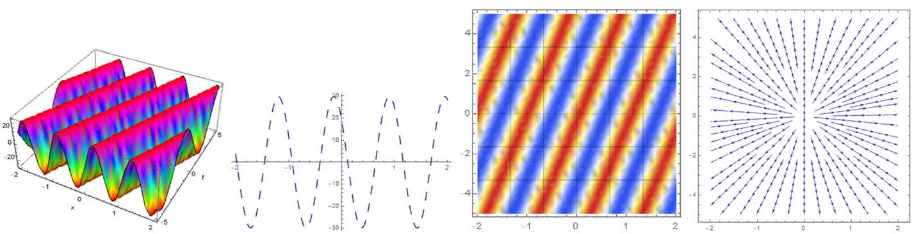

(a) **(b)** **(c)** **(d)**

Fig. 28 Graphical representation of solution $z_4(x,t)$ in Eq. (73) are presented via $a=5, \alpha=-0.5, c=0.3, d=2, p=3, v=0.5, \phi=0.2$

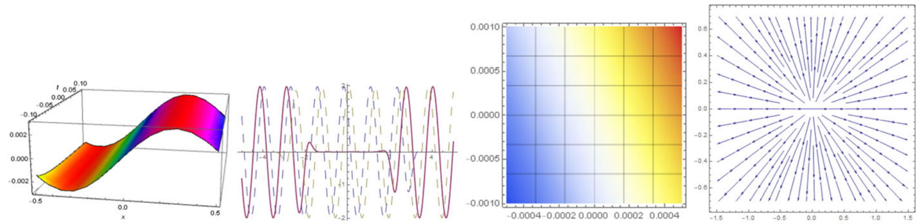

(a) (b) (c) (d)

Fig. 29 Graphical representation of solution $y_5(x,t)$ in Eq. (77) are presented via $u_5 = 7.5,\ a = 4, \alpha = -0.2, c = -6.7, d = 2.5, \eta = -5.5, p = -5, u = 2, u_2 = -0.06, u_3 = -3, u_4 = -1, v = 0.09, w_1 = 4, w_2 = 7, w_3 = 3.7,\ w_4 = -0.7, \psi = 8, z_1 = -1, z_2 = 3, \phi = 5$

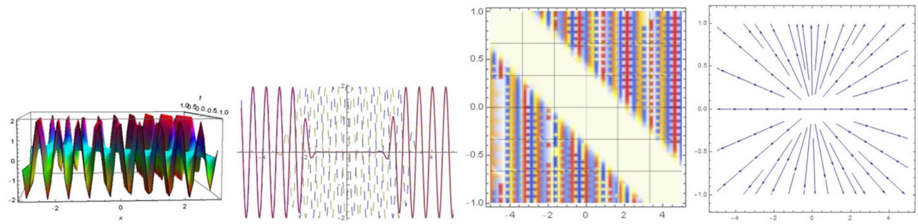

(a) (b) (c) (d)

Fig. 30 Graphical representation of solution $z_5(x,t)$ in Eq. (77) are presented via $u_5 = 7.5,\ a = 4, \alpha = -0.2, c = -6.7, d = 2.5, \eta = -5.5, p = -5, u = 2, u_2 = -0.06, u_3 = -3,$
$u_4 = -1, v = 0.09, w_1 = 4, w_2 = 7, w_3 = 3.7, w_4 = -0.7, \psi = 8, z_1 = -1, z_2 = 3, \phi = 5$

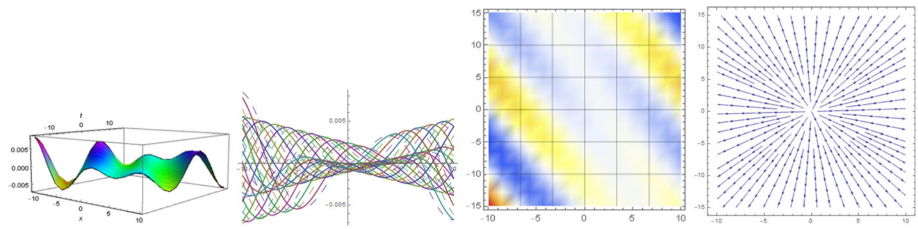

(a) (b) (c) (d)

Fig. 31 Graphical representation of solution $y_6(x,t)$ in Eq. (80) are presented via $a = 0.5, alpha = 0.08, c = 0.2, d = -0.4, \eta = 0.2, p = 0.5, u = -2, u_2 = 0.6,$
$u_4 = -0.4, v = -0.3, w_2 = 7, \psi = -0.5, z_1 = 0.9, \phi = 3$

$$\frac{\partial \Gamma_j}{\partial c} > 0 \tag{91}$$

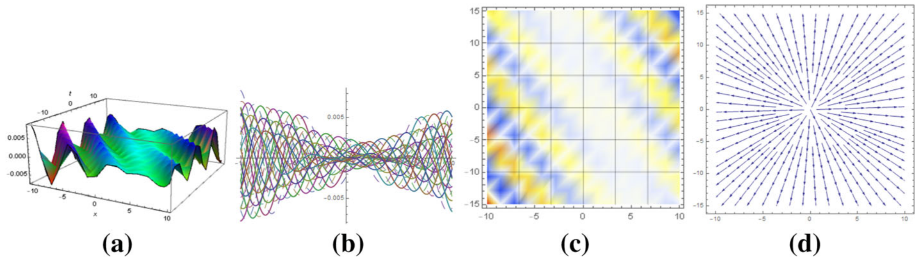

Fig. 32 Graphical representation of solution $z_6(x,t)$ in Eq. (81) are presented via $a=0.5, alpha=0.08, c=0.2, d=-0.4, \eta=0.2, p=0.5, \quad u=-2, u_2=0.6, u_4=-0.4, v=-0.3, w_2=7, \psi=-0.5, z_1=0.9, \phi=3$

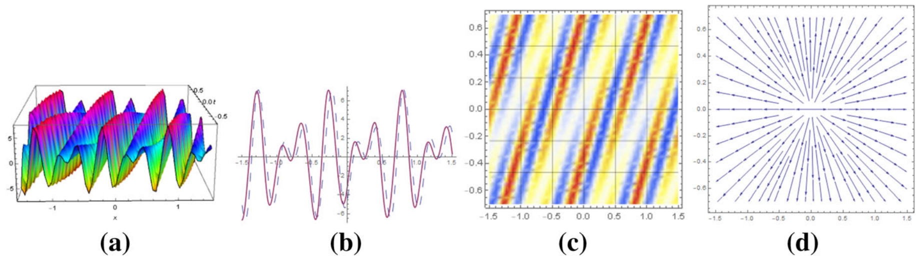

Fig. 33 Graphical representation of solution $y_7(x,t)$ in Eq. (84) are presented via $a=0.5, \alpha=8, c=0.2, d=0.4, \eta=-2, p=-3, \quad u=-2, u_2=-0.6, u_3=-0.3, u_4=0.7, u_5=-8, v=-3, w_2=5, w_3=-0.3, w_4=-7, \psi=-0.5, z_1=-0.9, z_2=-5, \phi=5$

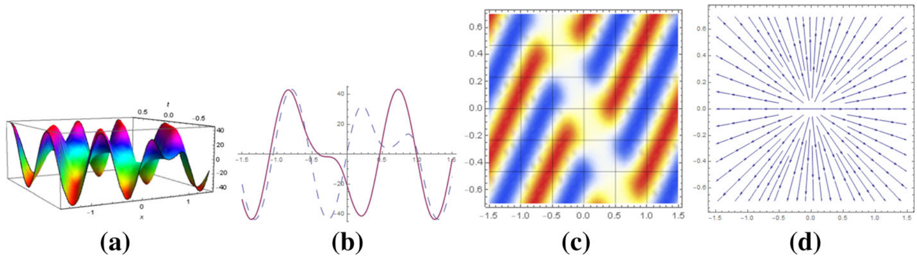

Fig. 34 Graphical representation of solution $z_7(x,t)$ in Eq. (85) are presented via $a=0.5, \alpha=8, c=0.2, d=0.4, \eta=-2, p=-3, \quad u=-2, u_2=-0.6, u_3=-0.3, u_4=0.7, u_5=-8, v=-3, w_2=5, w_3=-0.3, w_4=-7, \psi=-0.5, z_1=-0.9, z_2=-5, \phi=5$

where Γ_j (j=1,2) and c represented as momentum and velocity respectively (Figs. 21, 22, 23, 24, 25, 26, 27, 28, 29, 30, 31,32, 33,34, 35 and 36). Hamiltonian system provides the stability condition, all solutions we got through this condition is given by (Table 1), ,

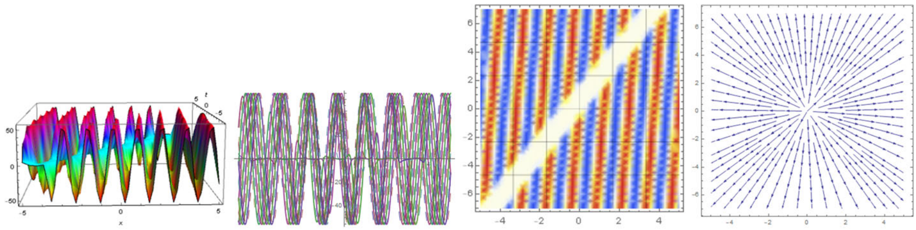

(a) (b) (c) (d)

Fig. 35 Graphical representation of solution $y_8(x,t)$ in Eq. (88) are presented via $a=-0.5, \alpha=8, c=0.2, d=0.4, \eta=-2, p=5, u=-2, u_2=0.6, u_3=-0.3, u_4=0.4, u_5=8, v=0.3, w_2=5, w_3=0.3, w_4=7, \psi=-0.5, z_1=-0.9, z_2=-5, \phi=3$

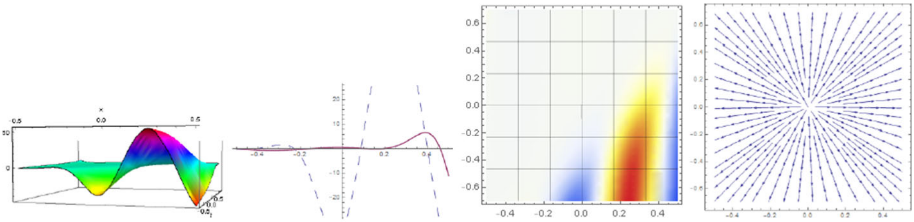

(a) (b) (c) (d)

Fig. 36 Graphical representation of solution $z_8(x,t)$ in Eq. (89) are presented via $a=-0.5, \alpha=8, c=0.2, d=0.4, \eta=-2, p=5, u=-2, u_2=0.6, u_3=-0.3, u_4=0.4, u_5=8, v=0.3, w_2=5, w_3=0.3, w_4=7, \psi=-0.5, z_1=-0.9, z_2=-5, \phi=3$

22 Results and discussion

By establishing the proper values for the parameters, we were able to successfully generate the desired type of solutions which express wave discrepancy. Take note of Figs. 1 and 2 which presents bright soliton solution for Eq. (7–8) by using appropriate values for parameters. In Figs. (a) 3D plot (b) 2D plot and (c) contour plot respectively. We get some multiple bright soliton graph for Eq. (11-12) by using the values $a_1=1.5, b_1=7, d_1=0.9, k_2=0.5, k_5=0.2, k_6=-4, k_7=-2, n_1=2.2, s=0.05$ in Figs. 3 and 4. The geometrical structures of lump wave soliton solutions are presented in Figs. 4, 5, 6, 7, 8, 9 and 10 for various values for parameters. Figures 13, 14, 15, 16, 17, 18, 19 and 20 shows kink type LSS for different values of parameters. We have computed M-shaped graphs for $y_1(x,t)$ and $z_1(x,t)$ with values $a=2, \alpha=0.8, c=0.01, d=-4, \eta=2, p=5, u=2, u_2=0.06, u_3=-0.03, u_4=-0.9, u_5=5, v=0.3, w_2=5, w_3=3, w_4=-7, \psi=8, z_1=0.9, z_2=-5, \phi=0.5$ in Figs. 21 and 22, (a) 3D plot (b) 2D plot (c) density plot and (d)

Table 1 Stability $y_i(x,t)$ and $z_i(x,t)$ where $(i = 1, 2, 3, ..., 8.)$

Solution	Stability	Values of variables
$y_1(x,t)$	Unknown	$a = 2, \alpha = 0.8, c = 0.01, d = -4, \eta = 2, p = 5, u = 2, u_2 = 0.06,$
$z_1(x,t)$	Stable	$u_3 = -0.03, u_4 = -0.9, u_5 = 5, v = 0.3, w_2 = 5, w_3 = 3, w_4 = -7, \psi = 8, z_1 = 0.9, z_2 = -5, \phi = 0.5$
$y_2(x,t)$	Stable	$a = -2, \alpha = -0.2, c = 10, d = 0.4, \eta = 5, p = 1.5, u = -2, u_2 = 0.6,$
$z_2(x,t)$	Stable	$u_3 = -3, u_4 = 1.9, u_5 = -0.5, v = -3, w_2 = 1.5, w_3 = 0.03, w_4 = -0.7, \psi = -0.8, z_1 = -0.1, z_2 = 5, \phi = 15.$
$y_3(x,t)$	Unknown	$a = -2.4, \alpha = -0.2, c = 1.7, d = 2.4, \eta = 5.5, p = 6.5, u = 2.5,$
$z_3(x,t)$	Unstable	$u_2 = -0.6, u_3 = -0.03, u_4 = -1.9, u_5 = 0.5, v = -3.9, w_1 = 0.4, w_2 = 1.05, w_3 = 3.7, w_4 = 0.7, \psi = 0.08,$ $z_1 = 0.01, z_2 = -3, \phi = 1.05.$
$y_4(x,t)$	Stable	$a = 5, \alpha = -0.5, c = 0.3, d = 2, p = 3, v = 0.5,$
$z_4(x,t)$	Unknown	$\phi = 0.2.$
$y_5(x,t)$	Unknown	$u_5 = 7.5, a = 4, \alpha = -0.2, c = -6.7, d = 2.5, \eta = -5.5, p = -5,$
$z_5(x,t)$	Unstable	$u = 2, u_2 = -0.06, u_3 = -3, u_4 = -1, v = 0.09, w_1 = 4, w_2 = 7, w_3 = 3.7, w_4 = -0.7, \psi = 8, z_1 = -1, z_2 = 3, \phi = 5.$
$y_6(x,t)$	Unknown	$a = 0.5, alpha = 0.08, c = 0.2, d = -0.4, \eta = 0.2, p = 0.5, u = -2,$
$z_6(x,t)$	Unknown	$u_2 = 0.6, u_4 = -0.4, v = -0.3, w_2 = 7, \psi = -0.5, z_1 = 0.9, \phi = 3.$
$y_7(x,t)$	Stable	$a = 0.5, \alpha = 8, c = 0.2, d = 0.4, \eta = -2, p = -3, u = -2,$
$z_7(x,t)$	Unknown	$u_2 = -0.6, u_3 = -0.3, u_4 = 0.7, u_5 = -8, v = -3, w_2 = 5, w_3 = -0.3, w_4 = -7, \psi = -0.5, z_1 = -0.9, z_2 = -5, \phi = 5.$
$y_8(x,t)$	Unstable	$a = -0.5, \alpha = 8, c = 0.2, d = 0.4, \eta = -2, p = 5, u = -2,$
$z_8(x,t)$	Unstable	$u_2 = 0.6, u_3 = -0.3, u_4 = 0.4, u_5 = 8, v = 0.3, w_2 = 5, w_3 = 0.3, w_4 = 7, \psi = -0.5, z_1 = -0.9, z_2 = -5, \phi = 3.$

stream plot respectively. Figures 23 and 24 represented graph of M-shaped with one and two kinks. We have attained the breather for $y_4(x,t)$ and $z_4(x,t)$ with values $a=5, \alpha=-0.5, c=0.3, d=2, p=3, v=0.5, \phi=0.2$ in Figs. 27 and 28. We also obtained some M-shaped interaction with periodic, rogue and kink profiles are presented in Figs. 29, 30, 31, 32, 33, 34, 35 and 36.

23 Conclusion

In this paper, we explored distinct solutions for NLSE-QNS such as multi, rogue and periodic waves. we have investigated lump with kink, lump periodic and kink, breather lump, homoclinic breather. We also categorised *MSRS*, *MSRS* with one and two kink, *HBS*, *PCRS*, *KCRS*, *MSPK* and *MSRK*. Additionally, we also manipulated their stability. We discovered by HS properties that $y_i(x,y)$, $z_j(x,y)$ where $(i=2,4,7)$ and $(j=1,2)$ to be stable solutions.

Funding Not applicable.

Availability of data and materials Not applicable.

Declarations

Conflict of interest The authors declare no conflict of interest.

Ethical approval I hereby declare that this manuscript is the result of my independent creation under the reviewers' comments. Except for the quoted contents, this manuscript does not contain any research achievements that have been published or written by other individuals or groups.

References

Ahmed, I., Seadawy, A. R., Lu, D.: *M*-shaped rational solitons and their interaction with kink waves in the Fokas–Lenells equation. Physica Scripta **94**, 055205 (2019)

Ahmed, I., Seadawy, A.R., Lu, D.: Kinky breathers, W-shaped and multi-peak solitons interaction in $(2+1)$-dimensional nonlinear Schrödinger equation with Kerr law of nonlinearity. Eur. Phys. J. Plus **134**(3), 1–10 (2019)

Ali, K., Seadawy, A.R., Ahmad, S., Rizvi, S.T.R.: Discussion on rational solutions for Nematicons in liquid crystal with Kerr law. Chaos Solitons Fract. **160**, 112218 (2022)

Ashraf, F., Seadawy, A.R., Rizvi, S.T.R., Ali, K., Ashraf, M.A.: Multi-wave, M-shaped rational and interaction solutions for fractional nonlinear electrical transmission line equation. J. Geom. Phys. **177**, 104503 (2022)

Batool, T., Rizvi, S.T.R., Seadawy, A.R.: Multiple breathers and rational solutions to Ito integro-differential equation arising in shallow water waves. J. Geom. Phys. **178**, 104540 (2022)

Biswas, A., Ekici, M., Khan, S., Triki, H., Moraru, L., Alzahrani, A.K.: Embedded solitons with $\chi^{(2)}$ nonliniearity susceptibility. Scientia Iranica (2022). https://doi.org/10.24200/SCI.2022.55560.4276

Guo, J.-L., Yang, Z.-J., Song, L.-M., Pang, Z.-G.: Propagation dynamics of tripole breathers in nonlocal nonlinear media. Nonlinear Dyn. **101**, 1147–1157 (2020)

Ilhan, V., Manafian, J., Lakestani, M., Singh, G.: Some novel optical solutions to the perturbed nonlinear Schrödinger model arising in nano-fibers mechanical systems. Mod. Phys. Lett. B **36**(03), 2150551 (2022)

Khater, A.H.: Computational simulations. Propagation behavior of the Riemann wave interacting with the long wave. Ocean Eng. **153**, 281–296 (2019)

Li, X., Manafian, J., Abotaleb, M., Ilhan, O., Oudah, A.Y., Prakaash, A.S.: Novel optical soliton waves in metamaterials with parabolic law of nonlinearity via the IEFM and ISEM. J. Funct. Spaces **2022**, 1 (2022). https://doi.org/10.1155/2022/1351377

Manafian, J., Ivatloo, M., Abapour, B.M.: Breather wave, periodic, and cross-kink solutions to the generalized Bogoyavlensky–Konopelchenko equation. Math. Methods. Appl. Sci. **43**(4), 1753–1774 (2020)

Mohyaldeen, S.Y., Manafian, J., Ilhan, O.A., Abotaleb, M., Hajar, A.: Periodic and breather solutions for miscellaneous soliton in metamaterials model by computational schemes. Int. J. Geom. Methods Mod. Phys. **19**(12), 2250196 (2022)

Ren, B., Lin, J., Lou, Z.M.: A new nonlinear equation with lump-soliton, lump-periodic, and lump-periodic-soliton solutions. Complexity **2019**, 1–10 (2019)

Rizvi, S.T.R., Seadawy, A.R., Ahmed, S., Younis, M., Ali, K.: Study of multiple lump and rogue waves to the generalized unstable space time fractional nonlinear Schrödinger equation. Chaos Solitons Fract. **151**, 111251 (2021)

Rizvi, S.T.R., Seadawy, A.R., Raza, U.: Detailed analysis for chirped pulses to cubic-quintic nonlinear non-paraxial pulse propagation model. J. Geom. Phys. **178**, 104561 (2022)

Rizvi, S.T.R., Seadawy, A.R., Farrah, N., Ahmad, S.: Application of Hirota operators for controlling soliton interactions for Bose-Einstien condensate and quintic derivative nonlinear Schrödinger equation. Chaos Solitons Fract. **159**, 112128 (2022)

Seadawy, A.R., Bilal, M., Younis, M., Rizvi, S.T.R., Althobaiti, S., Makhlouf, M.M.: Analytical mathematical approaches for the double chain model of DNA by a novel computational technique. Chaos Solitons Fract. **144**, 110669 (2021)

Seadawy, A.R., Rizvi, S.T.R., Ahmad, S., Younis, M., Baleanu, D.: Lump, lump-one stripe, multiwave and breather solutions for the Hunter–Saxton equation. Open Phys. **19**(1), 1–10 (2021)

Seadawy, A.R., Rizvi, S.T.R., Ashraf, M.A., Younis, M., Hanif, M.: Rational solutions and their interactions with kink and periodic waves for a nonlinear dynamical phenomenon. Int. J. Mod. Phys. B **35**, 2150236 (2021)

Seadawy, A.R., Ahmad, S., Rizvi, S.T.R., Ali, K.: Various forms of lumps and interaction solutions to generalized Vakhnenko Parkes equation arising from high-frequency wave propagation in electromagnetic physics. J. Geom. Phys. **176**, 104507 (2022)

Seadawy, A.R., Rizvi, S.T.R., Mustafa, B., Ali, K., Althubiti, S.: Chirped periodic waves for an cubic quintic nonlinear Schrödinger equation with self steepening and higher order nonlinearities. Chaos Solitons Fract. **156**, 111804 (2022)

Seadawy, A.R., Younis, M., Baber, M.Z., Iqbal, M.S., Rizvi, S.T.R.: Nonlinear acoustic wave structures to the Zabolotskaya Khokholov dynamical model. J. Geom. Phys. **175**, 104474 (2022)

Seadawy, A.R., Akram, U., Rizvi, S.T.R.: Dispersive optical solitons along with integrability test and one soliton transformation for saturable cubic-quintic nonlinear media with nonlinear dispersion. J. Geom. Phys. **177**, 104521 (2022)

Shen, S., Yang, Z., Li, X., Zhang, S.: Periodic propagation of complex-valued hyperbolic-cosine-Gaussian solitons and breathers with complicated light field structure in strongly nonlocal nonlinear media. Commun. Nonlinear Sci. Numer. Simul. **103**, 106005 (2021)

Shen, S., Yang, Z.-J., Pang, Z.-G., Ge, Y.-R.: The complex-valued astigmatic cosine-Gaussian soliton solution of the nonlocal nonlinear Schrödinger equation and its transmission characteristics. Appl. Math. Lett. **125**, 107755 (2022)

Song, L.-M., Yang, Z.-J., Li, X.-L., Zhang, S.-M.: Coherent superposition propagation of Laguerre–Gaussian and Hermite-Gaussian solitons. Appl. Math. Lett. **102**, 106114 (2020)

Wang, M., Zhou, Y., Li, Z.: Application of a homogeneous balance method to exact solutions of nonlinear equations in mathematical physics. Phys. Lett. A **216**, 67–75 (1996)

Yang, J.Y., Ma, W.X., Qin, Z.: Lump and lump-soliton solutions to the (2+1)-dimensional Ito equation. Anal. Math. Phys. **8**(3), 427–436 (2018)

Yang, Z.-J., Zhang, S.-M., Li, X.-L., Pang, Z.-G., Hong-Xia, B.: High-order revivable complex-valued hyperbolic-sine-Gaussian solitons and breathers in nonlinear media with a spatial nonlocality. Nonlinear Dyn. **94**, 2563–2573 (2018)